UNCLASSIFIED

DEFENCE RESEARCH ESTABLISHMENT
CENTRE DE RECHERCHES POUR LA DÉFENSE
VALCARTIER, QUÉBEC

DREV - TR – 2000-115
Unlimited Distribution / Distribution illimitée

AERODYNAMIC CHARACTERISTICS OF THE BDU-5002/B MOD 1 BOMB AT SUBSONIC AND TRANSONIC VELOCITIES FROM AEROBALLISTIC RANGE FREE-FLIGHT TESTS

by

A. D. Dupuis

November/novembre 2000

Approved by/ approuvé par

Head, Delivery Systems Section
Chef, Section systèmes de lancement

3 Nov 00
Date

SANS CLASSIFICATION

WARNING NOTICE

The information contained herein is proprietary to Her Majesty and is provided to the recipient on the understanding that it will be used for information and evaluation purposes only. Any commercial use, including use for manufacture, is prohibited. Release to third parties of this publication or of information contained herein is prohibited without the prior written consent of DND Canada.

© Her Majesty the Queen in Right of Canada as represented by the Minister of National Defence, 2000

ABSTRACT

Free-flight tests were conducted in the Defence Research Establishment Valcartier (DREV) aeroballistic range on a full-scale MPB-LD (BDU-5002/B MOD 1) bomb from subsonic to transonic velocities. All the main aerodynamic coefficients and dynamic stability derivatives were very well determined using the six-degree-of-freedom single- and multiple-fit data reduction techniques. The cubic pitch moment and the cubic normal force coefficients terms, the yaw axial force term as well as induced moments were also reduced. Indraft wind tunnel and open jet facility experimental results were compared with the free flight ones. Estimates of the aerodynamic coefficients from two analytical codes and from one computational fluid dynamic analysis were compared with the free-flight results.

RÉSUMÉ

Des essais en vol libre ont été effectués dans le corridor aérobalistique du Centre de recherches pour la défense Valcartier (CRDV) avec la bombe en vraie grandeur MPB-LD (BDU-5002/B MOD 1) aux vitesses subsoniques et transsoniques. Tous les coefficients aérodynamiques principaux et les dérivés de stabilité dynamique ont été très bien déterminés grâce aux méthodologies de réduction à six degrés de liberté par les options de réduction simple et multiple. Les termes cubiques des coefficients du moment de tangage et de la force normale, le terme du deuxième ordre pour la force axiale ainsi que les moments induits ont aussi été réduits. Les résultats expérimentaux de la soufflerie à rafale et à veine libre sont comparées avec ceux obtenues en vol libre. L'estimation des coefficients aérodynamiques de deux méthodes analytiques ainsi que d'une analyse de l'écoulement des fluides ont aussi été comparées aux résultats des essais en vol libre.

REPRODUCTION QUALITY NOTICE

This document is the best quality available. The copy furnished to DRDCIM contained pages that may have the following quality problems:

: Pages smaller or Larger than normal

: Pages with background colour or light coloured printing

: Pages with small type or poor printing; and or

: Pages with continuous tone material or colour photographs

Due to various output media available these conditions may or may not cause poor legibility in the hardcopy output you receive.

☒ **If this block is checked, the copy furnished to DRDCIM contained pages with colour printing, that when reproduced in Black and White, may change detail of the original copy.**

102-00972/

TABLES OF CONTENTS

ABSTRACT/RÉSUMÉ i
EXECUTIVE SUMMARY v
NOMENCLATURE vii
1.0 INTRODUCTION 1
2.0 MODEL CONFIGURATION 4
2.1 MPB-LD Configuration 4
2.2 Sabot Design 5
3.0 FACILITY DESCRIPTION AND TEST CONDITIONS 6
3.1 DREV Aeroballistic Range 6
3.3 Test Conditions and Particularities 7
4.0 FREE-FLIGHT DATA REDUCTION 8
5.0 FREE-FLIGHT RESULTS AND DISCUSSIONS 10
5.1 Linear Theory Results 10
5.2 Six-Degree-of-Freedom Results 11
5.3 Comparison of 6DOF Single- and Multiple-Fit Results 13
5.4 Comparison of Aeroballistic Range and Other Experimental Results 16
6.0 AERODYNAMIC PREDICTION METHODOLOGIES 17
7.0 COMPARISON OF AEROBALLISTIC RANGE AND PREDICTED RESULTS 19
7.1 General Comments 21
8.0 CONCLUSIONS AND RECOMMENDATIONS 23
9.0 ACKNOWLEDGEMENTS 24
10.0 REFERENCES 25
TABLES I to IX
FIGURES 1 to 10
APPENDIX A - Angular Motion Plots
APPENDIX B - CFD Results
APPENDIX C - Comparison of All Results

EXECUTIVE SUMMARY

The CF has developed a Store Separation Model (SSM) to predict the separation of stores from the CF-18 aircraft given a configuration and initial conditions. This model was developed in order to reduce the risk of flight test incidents, and to reduce store separation work by directing efforts to critical areas. SSM has been used extensively by Canadair on behalf of DND to support various CF-18 stores clearance projects in the past. The current flight matching technique uses a trial and error approach, which is very time-consuming and costly. It was shown recently that the implementation of the Maximum Likelihood Method (MLM) in the SSM could resolve its inherent deficiencies. The MLM has the capability of extracting aerodynamic coefficients and interference parameters, simultaneously from measured store separation trajectories. The Ballistic SSM (BSSM), under development, would be able to predict full-scale separation and ballistic flight test data for the CF-18 aircraft.

Even though the MLM is a well-proven technique to extract interference coefficients and aerodynamic coefficients (static and dynamic), the store separation tests usually do not have enough angular and translational motion so that it can be utilized to its maximum efficiency. It is therefore required to have a very good free stream aerodynamic (static and dynamic) coefficient data base of stores dropped from the CF-18 to be able to extract the interference coefficients with a high degree of confidence. If the free stream aerodynamics of the store are in error, the MLM will over or under estimate the interference coefficients to fit the overall observed motion. This reliable free stream aerodynamic data base will also be used with the BSSM and the DREV 6DOF trajectory simulation program to predict accurate store impact at the target and in the CF-18 Ballistic Integrator Algorithm OFP.

DREV has a unique free - flight aeroballistic range where aerodynamic coefficients (static and dynamic) are reduced from measured trajectories with the MLM methodology. Projectiles (scaled or full scale) are fired from a powdered gun through 54 indirect shadowgraph stations. This aeroballistic range has shown over the years to be able to extract very reliable aerodynamic coefficients.

DREV was tasked by NDHQ to fire a first series of store configurations in the DREV aeroballistic range with the goal of obtaining their free stream static and dynamic aerodynamic coefficients. A second objective was to evaluate various available tools to predict the aerodynamic coefficients in view of reducing costs of experimental tests. The stores that were chosen for this first phase were: LDGP MK82 CF, BDU-5002/B Mod 1 (Modular Practice Bomb - Low Drag), and BDU-5003/B MOD 1 (Modular Practice Bomb - High Drag). The Mach number range of interest is between Mach 0.6 and 1.5.

This report presents the aerodynamic coefficients and stability derivatives that were deduced from free-flight tests conducted in the DREV aeroballistic range on a full-

scale BDU-5002/B Mod 1 (Modular Practice Bomb - Low Drag) bomb. All the main aerodynamic coefficients and dynamic stability derivatives as well as the nonlinear ones were determined using the six-degree-of-freedom single- and multiple-fit data reduction techniques. The cubic pitch moment, the cubic normal force coefficient terms, the yaw axial force term as well as induced moments were also reduced. Indraft wind tunnel and open jet facility experimental results as well as full-scale free-trials were compared with the aeroballistic range ones. The estimates of the aerodynamic coefficients from two analytical codes (PRODAS, and AP95) and from one computational fluid dynamic analyses were also compared with the free-flight results.

In general, the estimates provided for the MPB-LD computations were reasonable but there is not one individual code that could predict all the aerodynamic coefficients that are required with a high degree of confidence. Even though the absolute values of the estimates were off the experimental data, the trends of the estimated aerodynamic coefficients with Mach number, when compared with the experimental data, were very good. This seems to suggests that an astute combination of free-flight experimental data and the use of analytical and CFD tools could provide a reliable data base of aerodynamic coefficients and stability derivatives that would cover the Mach number and angle-of-attack range of interest.

This data base of aerodynamic coefficients generated by this experimental program is considered a success and it can be used with the BSSM, the SSM as well as the DREV 6DOF trajectory program to predict accurate weapon performance. Also, it can be exploited with confidence for the CF-18 OFP. The methodology should be extended to other weapon systems.

NOMENCLATURE

Variable	Computer Output	Description
A		Cross sectional area of projectile (m^2)
d		Diameter of projectile (mm)
c. g.	CG	Center of gravity (m)
C_{l_p}		Roll damping moment coefficient
$C_{l\delta}$		Roll moment coefficient due to fin cant
$C_{l\gamma}$	Clg	Induced roll moment coefficient
C_{np}	Cnp	Magnus moment coefficient
$C_{n\gamma}$	Cng	Induced yaw moment coefficient
C_{nsm}	Cnsm	Side moment coefficient
C_N	CN	Normal force coefficient
$C_{N\delta}\,\delta_A$	CNda	Trim force coefficient component
$C_{N\delta}\,\delta_B$	CNdB	Trim force coefficient component
C_M	Cm	Static pitch moment coefficient
C_{Mq}	Cmq	Pitch damping moment coefficient
$C_{M\delta}\,\delta_A$	Cmda	Trim moment coefficient component
$C_{M\delta}\,\delta_B$	CmdB	Trim moment coefficient component
$C_{m\gamma}$	Cmg	Induced pitching moment coefficient
C_{X0}	CX0	Axial force coefficient at zero angle of attack
C_{Yp}	CYp	Magnus moment coefficient
$C_{Y\gamma}$	CYg	Induced normal force coefficient
$C_{Z\gamma}$	CZg	Induced normal force coefficient

I_x, I_y	-	Axial and transverse moments of inertia (kg m^2)
l	-	Length of projectile (m)
l/d	-	Length-to-diameter ratio
m	-	Mass of projectile (kg)
M	Mach	Mach number
MPB-LD	-	Modular Practice Bomb - Low Drag
p	-	Spin rate (rad/s or deg/m)
Re_l	-	Reynolds number based on length of projectile
u, v, w	-	Projectile component velocities (m/s)
V	-	Total projectile velocity (m/s)
X, Y, Z	-	Projectile coordinates (m)
t	-	Time of flight (s)
$\bar{\alpha}$	a	Total angle of attack (deg)
$\bar{\alpha}_{max}$	AMAX	Maximum angle of attack (deg)
λ_N, λ_P	LN, LP	Nutation and precession damping (1/m)
θ, ψ, ϕ	-	Projectile orientation (deg)
δ	-	Fin cant angle (rad or deg)
δ_T	-	Total trim angle (rad or deg)
$\bar{\delta}^2$	DBSQ	Mean squared yaw (deg^2)
ε	-	Sine of the total angle of attack, $\sin\bar{\alpha} = \frac{v^2 + w^2}{V^2}$
ρ	-	Air density (kg/m^3)
6DOF	-	Six degree of freedom

Subscripts

$\overline{\alpha}_i$	ai (i)	Derivative with respect to ε_i
M	M	Variation with Mach number

Examples

$C_{M\overline{\alpha}}$	Cma	Pitching moment coefficient slope
$C_{M\overline{\alpha}3}$	Cma3	Pitching moment coefficient w.r.t. ε^3
$C_{Mq\overline{\alpha}_2}$	Cmq2	Pitch damping coefficient w.r.t.ε^2

1.0 INTRODUCTION

The CF has developed a Store Separation Model (SSM) to predict the separation of stores from the CF-18 aircraft given a configuration and initial conditions in order to reduce the risk of flight test incidents, and to reduce store separation work by directing efforts to critical areas. SSM has been used extensively by Canadair on behalf of DND to support various CF-18 stores clearance projects in the past. Because of inherent model limitations, it is essential to implement the capability to adjust aerodynamic coefficients from the SSM database to match model predictions with flight test data. The current flight matching technique uses an ineffective trial and error approach, which is very time-consuming and costly.

The Defence Research Establishment Valcartier (DREV) has successfully implemented a computerized system which uses the Maximum Likelihood Method (MLM) to iteratively extract aerodynamic coefficients and interference parameters, simultaneously from the trajectory of test articles in their aeroballistic range and open jet facility. The heart of this system consists of two computer programs known as the Aeroballistic Range Facility Data Analysis System (ARFDAS, Ref. 1) and Open Jet Facility Data Analysis System (OJFDAS, Ref. 2). OJFDAS, (Ref. 2), successfully showed that it was possible to extract store separation interference coefficients and free-stream aerodynamic coefficients (static and dynamic), simultaneously. Feasibility work, which confirmed the compatibility of the MLM algorithms with the SSM, was carried out under MLM Phase 1 efforts (Ref. 3).

A SSM and Ballistic Store Separation Model (BSSM) compatible MLM algorithm, known as the Store Separation Model Data Analysis System (SSMDAS), was tested, under Phase 1 (Ref. 3) efforts and confirmed the ability of MLM techniques to correctly adjust aerodynamic free stream and interference coefficients to match SSM/BSSM predictions to full-scale separation and ballistic flight test data for the CF-18 aircraft. Implementation of such an automated system will improve the accuracy and efficiency of

DND's SSM and BSSM for future store separation and ballistics work. Canadair has implemented the MLM in the SSM and BSSM (Ref. 4). The modified SSM and BSSM shall have the capability of using MLM techniques to achieve a match of SSM/BSSM predicted trajectories to actual observed separation and free-flight trajectory data of stores dropped from CF-18 aircraft during flight test.

Even though the MLM is a well-proven technique to extract interference coefficients and aerodynamic coefficients (static and dynamic), the store separation tests usually do not have enough angular and translational motion so that it can be utilized to its maximum efficiency. It is therefore required to have a very good free stream aerodynamic (static and dynamic) coefficient database of stores dropped from the CF-18 to be able to extract the interference coefficients with a high degree of confidence. If the free stream aerodynamics of the store are in error, the MLM will over compensate for this, which might lead to errors in the determined interference coefficients. This reliable free stream aerodynamic database will also be used with the BSSM to predict accurate store impact at the target and in the CF-18 Ballistic Integrator Algorithm OFP. An NRC report (Ref. 5) also states this requirement for a reliable aerodynamic data base: "In this component approach to store integration, the essential baseline information is the store free stream aerodynamics. The aircraft flow field, carriage loads, and launch characteristics are considered as interferences (not necessarily small) to the aerodynamic characteristic of the store. Hence, whether flight tests, ground tests, or computations are used, a well-established aerodynamic data base for the store itself should be obtained".

DREV has a unique free-flight aeroballistic range (Ref. 6 and 7) where absolute aerodynamic coefficients (static and dynamic) are readily obtainable from measured trajectories with the MLM methodology. Scaled or full-scale projectiles can be fired from a powdered gun through 54 indirect shadowgraph stations. This aeroballistic range has shown over the years to be able to extract very reliable aerodynamic coefficients.

DREV was tasked by NDHQ to fire a first series of store configurations in the DREV aeroballistic range with the goal of obtaining their free stream static and dynamic aerodynamic coefficients. A second objective was to evaluate various available tools to predict the aerodynamic coefficients in view of reducing the costs of experimental testing. The stores that were chosen for this first phase were: a scaled LDGP MK-82 CF (18.6%), a full-scale BDU-5002/B Mod 1 (Modular Practice Bomb - Low Drag, MPB-LD) and the BDU-5003/B Mod 1 (Modular Practice Bomb - High Drag, MPB - HD). The Mach number range of interest is between Mach 0.6 and 1.5.

This report presents the aerodynamic coefficients and stability derivatives that were deduced from free-flight tests measured trajectories conducted in the DREV aeroballistic range on a full-scale BDU-5002/B Mod 1 (Modular Practice Bomb - Low Drag) bomb. All the main aerodynamic coefficients and dynamic stability derivatives as well as the nonlinear ones were determined using the six-degree-of-freedom single- and multiple-fit data reduction techniques. The cubic pitch moment, the cubic normal force coefficient terms, the yaw axial force term as well as induced moments were also reduced. Indraft wind tunnel and open jet facility experimental results were compared with the free-flight ones. The estimates of the aerodynamic coefficients from two analytical codes (PRODAS, and AP95) and from one computational fluid dynamic analyses were also compared with the free-flight results.

This trials was performed at DREV in October 1998 and the analysis in February 1999, under Work Unit 3ec16, Improvement to CF-18 Ballistics Algorithms.

2.0 MODEL CONFIGURATION

2.1 MPB-LD Configuration

The full-scale MPB-LD was a proper candidate since its caliber (50.8 mm) was a suitable size to fire in the DREV aeroballistic range. Also, an extensive wind tunnel data base exists at DREV on this configuration and it was also tested at length from aircraft. This was also one of the configurations that was tested in the DREV open jet facility and used as a basis to validate the MLM methodology in obtaining store interference coefficients and free stream aerodynamic coefficients, simultaneously (Ref. 2).

The in-service MPB-LD configuration was used. The main dimensions are provided in Fig. 1 in caliber. The reference diameter is 50.8 mm. The only external geometry difference from the standard practice bomb is that the fins were rotated 45° from the locator holes, i.e. one pair of fins is in line with the locator holes. This was done so as to be able to launch them with the sabot that was designed (Ref. 8). The fumer cartridge was also replaced by a dummy one to keep the center of gravity and the mass as close as possible to the in service bomb.

The MPB-LD has a 1.35 cal ogive nose followed by a 4.07 cal cylindrical portion and the fins are placed at the end of an 2.48 cal extended boattail. A 0.58 cal rounded base concludes the projectile geometry. The fins have a 2.00 cal span and are of a clipped delta type. The fin leading edges are blunt with a thickness of 0.08 cal which reduced to 0.05 cal at the trailing edge. The fins have no cant to produce spin rate. The center of gravity of the tested projectiles was located at 3.94 caliber from the nose with the dummy cartridge in the projectile. The total length of the projectile is 8.52 cal.

The nominal physical properties of the model are given in Table I and the physical properties of each test projectile in Table II.

2.2 Sabot Design

Since the projectile had to be launched from a powdered gun to conduct tests in the DREV aeroballistic range, special sabots had to be designed to fire them. Since the model configuration in this case is fin stabilized, a smooth bore gun was utilized. The standard gun employed at DREV to fire fin stabilized projectiles of these dimensions in the aeroballistic range is a 110-mm smooth bore gun.

Several aspects have to be considered when designing sabots and models. They are: projectile configuration, total mass, sabot separation at the sabot trap located at 9.2 m from the muzzle at the aeroballistic range, muzzle velocity desired, gun accelerations, etc. The last three mentioned have to be consistent from round to round. In these tests, the highest muzzle velocity desired was approximately 510 m/s (Mach 1.5) and the lowest, 200 m/s (Mach 0.6).

The tail portion of the modular practice bombs is made of a polycarbonate material. Therefore, it is impossible to launch them with a base plate pusher sabot since the projectile would disintegrate at launch. The modular practice bombs have two locator holes situated close to the center of gravity (Ref.8) and a sabot design that would pull the projectile by these holes presented an interesting option.

Figure 2 shows a schematic of the sabot with the MPB-HD projectile inside it. The sabot for the MPB-LD is exactly the same. The detail drawings of the sabot are provided in Ref. 8. It is a two-petal sabot design made of aluminum. The lengths of the saw cuts on each side were adjusted to obtain adequate petal separation for the expected velocities. A sabot base seal pad was also used to prevent gas leakage past the sabot body. It has two pins at the front of the sabot to pull the projectile down the barrel. These pins were designed to fit the in-service MPB locator holes.

A pivot pin, which is in line with the saw cuts, was added to force the sabot opening at that point. A polycarbonate ring with a 5° angle is positioned at the aft end of the sabot. There are two reasons for this. The first one, is to have a good pressure seal between the sabot and the gun tube so as to be able to have a known shot start pressure which helps in having consistent muzzle velocities at the same propellant charge mass. The second reason is that, as the sabot leaves the gun tube, the high radial pressure acting on the rear ring relative to the front part, causes the pivoting action at the pivot point of the sabot petals.

A photograph of the sabot-model package as well as all the components is shown in Fig. 3. One should notice the roll pin placed on one of the model fins to permit measuring the roll orientation of the projectile when fired in the aeroballistic range. The total model-sabot mass is approximately 5.1 kg. The complete drawings of the sabot as well as the proof trials that were conducted to verify sabot-model integrity at launch can be found in Ref. 8.

3.0 FACILITY DESCRIPTION AND TEST CONDITIONS

3.1 DREV Aeroballistic Range

The DREV aeroballistic range (Refs. 6 and 7) is an insulated steel-clad concrete structure used to study the exterior ballistics of various free-flight configurations. The range complex consists of a gun bay, control room and the instrumented range (Fig. 4a). A massive blast wall is located in front of the building to stop sabot pieces and minimize vibrations transmitted to the range structure and instrumentation. Projectiles of calibers ranging from 5.56 to 155 mm, including tracer types, may be launched. Large caliber models have been fired up to Mach 7.

The 230-meter instrumented length of the range has a 6.1-m square cross section with a possibility of 54 instrumented sites along the range (Fig. 4b). For most of these tests, 41 of the stations were utilized. These sites house fully instrumented orthogonal shadowgraph stations that yield photographs of the shadow of the projectile as it flies down the range. The maximum shadowgraph window, an imaginary circle within which a projectile will cast a shadow on both reflective screens, is 1.6 meters in diameter. There are also four Schlieren stations (two operational for these tests) at the beginning of the range that yield high quality flow photographs. The range is also air conditioned to maintain a constant relative humidity of approximately 45%. The nominal operational conditions of the range are 20° C at standard atmospheric conditions. The spark source and reference point locations that were used were deduced from a standard survey. A dynamic calibration was conducted in the X, Y, X, θ and ψ coordinates.

3.2 Test Conditions and Particularities

Eleven (11) projectiles were fired during the aeroballistic range program with the 110-mm smooth bore gun with the HI-LO adapter (Ref. 8). All the projectiles had roll pins. The range conditions for each test projectile at time of firing are indicated in Table III. The muzzle velocities range from a low of 230 m/s (Mach 0.6) to a maximum of 344 m/s (Mach 1.01) which yielded Reynolds number, based on the length of projectile, between 6.2×10^6 and 9.8×10^6, respectively. The angles of attack ranged from a low of 0.7° to a maximum of 12.0°.

The gun muzzle was situated at a downrange coordinate of approximately 6.32 m in the aeroballistic range coordinate system. Due to the low muzzle velocities, the movable butt was utilized to capture the projectiles before the end of the range. It was placed after the 47th shadowgraph stations at approximately 150.0 m. This allowed a possibility of 41 shadowgraph stations, or 115.0 m, to measure data. This butt was used

for 10 of the 11 projectiles. The full complement of stations (54) was used for one of the models fired at the highest muzzle velocity.

Due to the length of the models, the total shadow of the projectiles in flight could not be captured on the films. A time delay was deliberately set so that at least the base of the model could be seen with certainty. This allowed the reading of the films at the front and back of the fins for calculating the trajectory. It was expected that this would cause some errors in the data reductions due to the small-scale length. It is not believed that this significantly affected the reduced aerodynamic coefficients.

A typical Schlieren photograph showing the complex flow and shock structure of a projectile in flight can be seen in Fig. 5 for shot B09 at Mach 0.94.

The numbering scheme to refer to the shots and a particular configuration is as follows. The shot numbers are identified by one letter followed by 6 digits, as for example B981002. The letter corresponds to a particular configuration. The first four numbers (9810) indicate the date (year and month) that the projectile was fired in the range. The last two digits correspond to the shot number for that particular configuration. For the example given above, the shot number corresponds to the second shot of the Model B configuration that was fired in the range in October 1998. For convenience, the shot numbers are usually referred to the letter and the shot number, B02.

4.0 FREE-FLIGHT DATA REDUCTION

Extraction of the aerodynamic coefficients and stability derivatives is the primary goal in analyzing the trajectories measured in the DREV aeroballistic range. This was done by means of the Aeroballistic Range Facility Data Analysis System (ARFDAS, Ref. 1) described in Fig. 6. These programs incorporate a standard linear theory and a six-degree-of-freedom (6DOF) numerical integration technique. The 6DOF routine

incorporates the Maximum Likelihood Method (MLM) to match the theoretical trajectory with the experimentally measured trajectory. The MLM is an iterative procedure that adjusts the aerodynamic coefficients to maximize a likelihood function. The application of this likelihood function eliminates the inherent assumption in least square theory that the magnitude of the measurement noise must be consistent between parameters (irrespective of units). In general, the aerodynamic coefficients are nonlinear functions of angle of attack, Mach number and roll angle.

ARFDAS represents a complete ballistic range data reduction system capable of analyzing both symmetric and asymmetric models. The essential steps of the data reduction system are to (1) assemble the dynamic data (time, position, angles), model measured physical properties and atmospheric conditions, (2) perform linear theory analysis, and (3) perform 6DOF analysis.

These three steps have been integrated into data analysis system to provide the test scientist with a convenient and efficient means of interaction. At each step in the analysis, permanent records for each shot are maintained so that subsequent analyses with data modification are much faster.

The 6DOF data reduction system can also simultaneously fit multiple data sets (up to five) to a common set of aerodynamics. Using this multiple-fit approach, a more complete range of angle of attack and roll orientation combinations is available for analysis than would be available from a single flight. This increases the accuracy of the determined aerodynamic coefficients over the entire range of angles of attack and roll orientations.

The aerodynamic data presented in this report were obtained using the fixed-plane 6DOF analysis (MLMFXPL) with both the single- and multiple-fit data correlation techniques. The equations of motion have been derived in a fixed-plane coordinate system

with Coriolis effects included. The formal derivation of the fixed-plane model is given in Ref. 9.

All the results given here were reduced after the dynamic calibration biases were accounted for the X, Y, X, θ and ψ coordinates. The methodology of the dynamic calibration for the DREV aeroballistic range is explained in Ref. 10.

5.0 FREE-FLIGHT RESULTS AND DISCUSSIONS

The aerodynamic coefficients and stability derivatives that were reduced from the free-flight trajectories measured in the aeroballistic range are presented in tabular form for the linear theory analysis and in both tabular and plotted format for the 6DOF reductions. All of the determined aerodynamic coefficients are given at the mid-range measured Mach number. Shot B07 is not presented in these results since it is believed the experimental data was in error. There was no roll data for two shots, B10 and B11.

5.1 Linear Theory Results

The linear theory parameters deduced from the decoupled motion are provided in Table IV. The magnitudes of the angles of attack varied from a low of 0.7° to a high of roughly 12.0°. The amplitude of the initial nutation and precession arms, KF and KS, and the mean squared yaw (Dbsq) provides an indication of these angles of attack.

In all the cases the shots were dynamically stable as observed by the negative nutation and precession damping modes (LF and LS). The frequencies (WF and WS) are consistent, except for two shots (B09 and B12) where the angles of attack were extremely small. It should be noted that the trim angles (KT) are quite appreciable in some cases, of the order of 1.5°. This will be further investigated in the 6DOF analysis.

The aerodynamic coefficients deduced from the linear theory parameters are presented in Table V. The methodology to obtain the aerodynamic coefficients is explained in Ref. 1. The main aerodynamic coefficients (C_{X0}, $C_{N\alpha}$, $C_{M\alpha}$, C_{lp} and $C_{l\delta}\delta$) are consistent. There is some variation in C_{Mq} and this occurs mostly when the angles of attack were quite low, and this was expected in these cases. Except for one shot (B09, low angles of attack), all the models were statically and dynamically stable, as shown by the negative sign of the pitching moment coefficient slope and the pitch damping coefficient.

The standard deviation error in the angular motion (E-Ang) from the linear theory analysis (Table V) is quite high in some cases, and it occurs mostly for shots at high angles of attack. This suggests that the linear theory analysis was not fitting some parameters adequately, probably due to nonlinear variation with angle of attack in some aerodynamic coefficients. These nonlinearities, if they exist, are best modeled and reduced with the 6DOF reduction technique of the next section.

5.2 Six-Degree-of-Freedom Results

The determined aerodynamic coefficients, their standard deviation errors, and the standard deviation errors between the theoretical and experimental trajectories for the axial, angular and roll motions are given in Tables VI and VII for the single- and multiple-fit data reduction techniques, respectively. The moment reference center for the pitch and moment coefficients was at 46.0% of the length from the nose of the projectile (3.92 cal). All the results are given at the mid-range Mach number for the single-fit data reductions and at the average mid-range Mach numbers for the multiple-fit data reductions.

A coefficient that appears with a value and a (*) between parentheses directly below, indicates that this coefficient was held constant and one that has a (-) between parentheses indicates that this coefficient was solved for and that the standard deviation error for this coefficient was higher than 100%, that is, it does not influence the fit and it is considered undetermined. Those with numbers between parentheses represent the standard deviation error for that particular coefficient.

The multiple-fit groups were chosen by Mach numbers and three groups of multiple-fit data reductions were conducted, as given in Table VII.

As seen from the Tables VI and VII, all of the main aerodynamic coefficients (C_{X0}, $C_{N\alpha}$, $C_{M\alpha}$ and C_{Mq}) were very well determined, as indicated by the low probable errors of fits on the coefficients. Since there were no fin cant on the projectiles, the roll motion was very limited. Therefore, the roll damping moment, C_{lp}, was kept constant at the estimate values obtained from PRODAS (Ref. 11) and the roll producing moment due to fin cant, $C_{l\delta}\delta$, was allowed to vary to take into account any manufacturing tolerances in the fin angles. The aerodynamic trims for the pitch moment and the normal force were solved for all the shots. The cubic pitch moment coefficient expansion term ($C_{M_{\alpha^3}}$) was well determined in the single- and multiple-fit data reductions at Mach 0.7 and 0.85 where the angles of attack were appreciable. At low angles of attack the single fit $C_{M_{\alpha^3}}$ were held constant at the determined multiple-fit value. The yaw axial force ($C_{X_{\alpha^2}}$) and the cubic normal force expansion term ($C_{N_{\alpha^3}}$) were also well determined at Mach 0.7 in the multiple-fit data reduction and the respective single fits were held constant at the multiple-fit determined value at this Mach number. An induced side moment ($C_{n\gamma\alpha_3}$) was resolved as well at Mach 0.7 from the multiple data reduction.

The standard deviation errors of the single and multiple fits are of the order of 0.7 mm in the downrange coordinate, 1.2 mm in the swerve motion, 0.35° in pitch and yaw and of the order of 1.0° in roll. These errors of the fits in pitch and yaw and in the swerve direction are a bit high when compared with other test programs conducted in the DREV aeroballistic range. This is probably due to the special film reading technique that was used, as mentioned previously. The 6DOF probable errors of fits are smaller than the linear theory ones because of the better mathematical modeling of the motion, such as the inclusion of aerodynamic trims, angle of attack dependent terms and variations with Mach number.

5.3 Comparison of 6DOF Single- and Multiple-Fit Results

Comparisons of the reduced aerodynamic coefficients from the 6DOF data reduction techniques with the single- and multiple-fit results are given in Figs. 7. The single-fit data points (AB - SF) are shown as open circles while the multiple-fit data reduction results (AB - MF) are given as solid circles.

Appendix A presents, for every test shot, the total angle of attack history with the observed angular motion and the theoretical determined one with the reduced aerodynamic coefficients. The experimental data points (open circles) and the calculated trajectory (continuous line) from the determined coefficients are compared. This allows a verification that the reduced aerodynamic coefficients do fit the experimental trajectory satisfactorily. For every shot, the total angle of attack and the angular motion plots in pitch and yaw are given as a function of the downrange coordinate.

The axial force coefficient at zero angle of attack (C_{X0}) as a function of Mach number is shown in Fig. 7a. The subsonic C_{X0} is of the order of 0.25 with a slight

increase as the Mach number increases and it is 0.56 at Mach 1.02. The agreement is excellent between the single and the multiple fits.

$C_{N\alpha}$, the normal coefficient slope, versus the Mach number is displayed in Fig. 7b. There is a slight scatter in the single-fit results due to some low angle of attack cases. $C_{N\alpha}$ is about 8.0 over the whole Mach number range tested. The cubic normal force expansion term ($C_{N_{\alpha^3}}$) was -60.0 at Mach 0.71 (Fig. 7c).

The variation of the pitching moment coefficient slope, $C_{M\alpha}$, and the cubic expansion term $C_{M_{\alpha^3}}$ with Mach number are shown in Fig. 7d and Fig. 7e, respectively. There is small scatter in the single fit results for $C_{M\alpha}$. The static stability increases as the Mach number increases, from -10.0 at Mach 0.65 to -16.0 at Mach 1.01. One interesting fact is that $C_{N\alpha}$ is constant over the same Mach number range. This implies that the center of pressure moves backwards quite significantly as the Mach number increases. $C_{M_{\alpha^3}}$ is of the order -260.0 at all Mach numbers. It should be noted that the shots at Mach 1.05 were all at low angles of attack (< 3.0°) and it was assumed that the cubic term would be the same as the other Mach numbers, for completeness.

The determined pitch damping coefficient, C_{Mq}, as a function of Mach number is presented in Fig. 7f. The pitch damping is in the region of -200 at Mach 0.7 and the damping increases almost linearly with the Mach number to reach -350 at Mach 1.05. The scatter is due to the shots that had low angles of attack.

C_{l_p}, the roll damping coefficient, is demonstrated versus the Mach number in Fig. 7g. This term was not solved for due to the lack of roll motion. These are the predicted values from PRODAS (Ref. 11) and it is about - 3.9.

The trim moment and trim normal force coefficients were well determined (Table VI) and they improved the fit noticeably when they were included in the fitting process. The asymmetries caused by modular design of the MPB-LD and the manufacturing tolerances contribute mostly to these coefficients. A trim angle can be calculated separately from the force and the moment term. The total moment trim is:

$$C_{M\delta}\delta_T = \sqrt{(C_{M\delta}\delta_A)^2 + (C_{M\delta}\delta_B)^2}$$

and the total trim angle is calculated as:

$$\delta_T = \arcsin\left(\frac{C_{M\delta}\delta_T}{C_{M\alpha}}\right)$$

The force trims are calculated in the same manner. The trend of the total trim angle from the force and moment calculations is shown in Fig. 7h versus the Mach number and, interestingly enough, the magnitudes are basically identical at the same Mach number. Usually, the trim moments are better resolved than the normal force trims. In most cases the trim angles are roughly 0.3° and for two shots the trim angles are 1.2°. The scatter in the results is also expected since no two bombs will be exactly the same.

The variation of C_M as a function of the angle of attack for the tested Mach numbers is shown in Fig. 8 for the multiple-fit data reductions. The maximum angles of attack observed in the aeroballistic range were in between 0.7° and 12.0°. In two cases, at Mach 0.70 and 0.85 the maximum angles of attack were 12.0° and 8.0°, respectively, and the cubic term was very well reduced. All the shots at Mach 1.02 had very low angles of attack 2.0° and since $C_{M_{\alpha^3}}$ could not be determined, it was assumed that the nonlinear variation would be similar to the other two cases. Therefore, for this case, C_M is basically extrapolated above 2.0°.

5.4 Comparison of Aeroballistic Range and Other Experimental Results

The MPB-LD was extensively tested in the DREV indraft wind tunnel (Ref. 12) during the design phase of the project and as well from full-scale aircraft free-flight trials (Ref. 13). The MPB-LD was also one of the configurations that was utilized in the open jet facility (Ref. 2) that successfully showed that it was possible to extract store separation interference coefficients and free stream aerodynamic coefficients (static and dynamic), simultaneously with the MLM methodology.

The reference center of gravity for the moment coefficient was taken to be the aeroballistic range one, that is 3.94 cal from the nose. The tabulated data from the indraft wind tunnel, open jet facility and from the full-scale free-flight trials can be found in Table VIII. The aerodynamic coefficients measured from the four experimental techniques; the aeroballistic range (AB-SF, AB-MF), the DREV indraft wind tunnel (WT), the open jet facility (OJF) and the full-scale tests (FF - M2470); are compared in Fig. 9. The full-scale tests only provided the total drag coefficient.

The axial force coefficient at zero angle of attack, C_{X0}, is compared in Fig. 9a versus the Mach number. The wind tunnel data agrees extremely well with the aeroballistic range data from Mach 0.7 to 0.9. The full-scale C_{X0} results are slightly above the aeroballistic range ones by 17% over the whole Mach number range tested. The trend with Mach number corresponds extremely well with the aeroballistic range one. The open jet facility point at Mach 0.88, lies above the aeroballistic range data by 37%.

$C_{N\alpha}$, the normal coefficient slope, versus the Mach number is displayed in Fig. 9b for three of the experimental techniques. The indraft wind tunnel and open jet facility data is within the scatter of the aeroballistic range results.

The variation of the pitching moment coefficient slope, $C_{M\alpha}$, with Mach number is shown in Fig. 9c. The lone open jet facility data point agrees very well with the aeroballistic range data, while the wind tunnel results indicate 15% more static stability. The wind tunnel Mach number trend is similar to the free-flight one. Since the wind tunnel $C_{N\alpha}$ agreed with the aeroballistic range data and $C_{M\alpha}$ does not, this implies that the wind tunnel center of pressure is further aft the aeroballistic range one.

6.0 AERODYNAMIC PREDICTION METHODOLOGIES

For design and evaluation purposes, it is necessary to have dependable tools to be able to predict quickly the aerodynamic performance of various projectile configurations. Also, to evaluate the performance of various weapon systems, 6DOF trajectory simulations are usually required and even desirable. This implies that a minimum of aerodynamic coefficients are required and these are: C_{X0}, $C_{N\alpha}$, $C_{M\alpha}$, C_{Mq}, C_{l_p} and $C_{l\delta}\delta$. These are usually provided as a function of Mach number.

The aerodynamic database on finned projectiles is quite established. The accessible codes are constantly being updated as the experimental data becomes available. These tools also have to be constantly validated with reliable experimental data to increase the confidence level when using them. The aerodynamic predictions from two of these analytical codes (PRODAS and AP95) were evaluated in this report. Also, a Navier-Stokes CFD analysis was also conducted, but it can only predict the values for C_{X0}, $C_{N\alpha}$, $C_{M\alpha}$. A short description of each code is given and the predictions are compared with the aeroballistic range experimental results in the next chapter.

The first aerodynamic predictions were made using the empirical and analytical techniques and tools from PRODAS (PROjectile Design Analysis System, Ref. 11). PRODAS is an interactive tool used to design and analyze various aspects of a weapon system efficiently and quickly, including projectile (spin and fin-stabilized) modeling, mass properties, aerodynamic coefficient estimation, stability analysis, internal ballistics, trajectory simulation and so on. It is an integrated system with a common data base and it was developed using proven methodologies and techniques so that the predicted performance estimates are based in part on prior experimental testing. The aerodynamic predictions were obtained from the stability portion of this program.

The aerodynamic predictions of AP-95 (AeroPrediction code 1995, Ref. 14) were also evaluated for this configuration. This code calculates static and dynamic aerodynamic coefficients for several classes of asymmetric, wing-body-tail configurations. Its basic methodology is that of component superposition where the body alone, lifting surface alone and interference contributions are summed to obtain the total configuration aerodynamics.

The CFD estimated aerodynamic coefficients were conducted by SNC TEC (Ref. 15) with the Tascflow code (Ref. 16) at the atmospheric conditions that were present in the aeroballistic range and at similar Mach numbers. Calculations were conducted at Mach numbers of 0.5, 0.8, 0.9, 1.1 and 1.5 and at angles of attack of 0.0°, 1.0°, 5.0°, 7.5° and 10.0°. A total of approximately 610 000 nodes were utilized to characterize the model and the flow field which extended beyond the base. The CFD tabulated results are presented in Appendix B as well as in graphical form. Since the aeroballistic range data and the CFD estimates for C_N and C_M showed some variation with angle of attack, a fit of the CFD data was conducted as follows:

$$C = a_0 \sin(\alpha) + a_1 \sin^3(\alpha)$$

a_0 and a_1 were solved for to obtain the first and third order expansion terms for the normal force coefficient C_N ($C_{N\alpha}$ and $C_{N_{\alpha^3}}$) and the pitch moment coefficient C_M ($C_{M\alpha}$ and $C_{M_{\alpha^3}}$). These calculated values are reported in Table IX. The axial force coefficient in the table is at zero angle of attack.

7.0 COMPARISON OF AEROBALLISTIC RANGE AND PREDICTED RESULTS

The aerodynamic predictions from PRODAS, AP-95 and the Navier-Stokes analyses are compared in Fig. 10 with the free-flight determined aerodynamic coefficients from the aeroballistic range. The reference center-of-gravity location of the tested projectiles (3.94 cal from nose) was utilized in the calculations for the aerodynamic moment predictions. The free-flight results from both the single- (AB-SF) and multiple-fit (AB-MF) are provided.

The PRODAS approximations for C_{X0} agree quite well in the subsonic and transonic region, except for a small section in between Mach numbers of 0.85 and 0.95 where it slightly overestimates the free-flight data (Fig. 10a). The AP95 C_{X0} is 30% below the test data between Mach 0.6 and 0.8 and the transonic trend with Mach number is not quite as steep as the experimental data. The CFD results for C_{X0} over predict the trial data by 50% over the whole Mach number range tested, but it agrees quite well with the PRODAS results supersonically.

The comparison for the normal force coefficient slope ($C_{N\alpha}$) is shown in Fig. 10b. The PRODAS approximations agree relatively well with the aeroballistic range data. The CFD assessment is above the multiple-fit data by about 16% but just outside the

experimental scatter of the single fit results. The AP95 predicted $C_{N\alpha}$ is below the test data by 50% over the whole Mach number range.

The $C_{M\alpha}$ comparison versus Mach number is shown in Fig. 10c. It easily seen the estimates from the CFD and PRODAS programs tremendously predict more static stability than the free-flight results by about 50% and 40%, respectively, while the AP95 calculations show less static stability by roughly a factor 2.0 to 2.5 when compared with the test data. Since the PRODAS and CFD predictions for $C_{N\alpha}$ were quite reasonable, this implies that the center of pressure location is very badly predicted by these codes to provide such estimates for $C_{M\alpha}$. The Mach number trend of the PRODAS estimates is good.

A comparison of C_M as a function of angle of attack is provided in Fig. 10d for the CFD estimates and the experimental data. The experimental data is shown at the three multiple nominal Mach numbers of 0.705, 0.853 and 1.02. PRODAS does not provide nonlinear estimates for the pitch moment coefficient and therefore it is not included in these assessments and no calculations were conducted with AP95. The CFD results at Mach 1.02 agree rather well with the test data at the higher angles of attack. At Mach 0.85, The CFD data agrees exactly with the experimental data at 10.0° yaw, but has a slightly different trend at the lower angles of attack. The same comments hold for the data at Mach 0.7. Overall, even though the slopes ($C_{M\alpha}$) are not well predicted by the CFD analyses (Fig. 10c), the overall trend at the higher angles of attack are quite acceptable.

The pitch damping coefficient, C_{Mq}, comparison is presented in Fig. 10e. There are no CFD results for the dynamic stability derivatives. For this coefficient, PRODAS predicts the right pitch damping coefficients between Mach numbers of 0.6 to 0.90 but it under predicts the test C_{Mq} by 30% in the transonic region. The subsonic AP95 estimates

below Mach 0.80 are reasonable but the approximations past that Mach number are very poor.

The C_{l_p} (roll damping coefficient) assessment is shown in Fig. 10f. As mentioned previously, due to a lack of roll motion since there were no fin cants on the projectiles, the experimental C_{l_p} was held constant at the PRODAS estimates and the roll moment producing term $C_{l\delta}\delta$ was solved for. This allowed very good fits in the roll motion, as witnessed in the standard deviation errors in the roll motion of Tables VI and VII. For this reason, the PRODAS estimates and the experimental data are the same. The AP95 under-predicts the former two by 35% over the whole the Mach number of interest.

For completeness purposes, all the results from the aeroballistic range, indraft wind tunnel, open jet facility and full-scale free-flight tests and the predicted values for C_{X0}, $C_{N\alpha}$ and $C_{M\alpha}$ are shown on the same graph in Appendix C. No further comments are provided since the full comparisons were conducted above.

7.1 General Comments

None of the predictive tools used in this analysis provided adequate absolute values for all the aerodynamic coefficients (C_{X0}, $C_{N\alpha}$, $C_{M\alpha}$, C_{Mq}, C_{l_p} and $C_{l\delta}\delta$) that would be necessary to conduct reliable 6DOF trajectory simulations, either in the SSM or BSSM models or as inputs to the CF-18 OFP. In some instances, in a particular Mach number range and at an angle of attack level, the agreement between the estimates and the test data was adequate. Not one particular code can be used to obtain reliable estimates, but a combination of them could be used. This is an easy statement after comparing with the experimental data, but a priori, and without reliable experimental data, it would be very difficult to chose one code that would achieve the goal, at least for configurations of

the MPB-LD type. The CFD calculations did provide more insight than the three analytical methods, especially for the angle of attack trend for C_M, but its major drawback is that it is limited to only static aerodynamic coefficients, namely, C_{X0}, C_N and C_M.

On the other hand and in many circumstances, even though the absolute values of the estimates were quite off the experimental data, the trends of the estimated aerodynamic coefficients with Mach numbers, when compared with the experimental data, were very good. This seems to suggests that an astute combination of free-flight experimental data and the use of the analytical tools could provide a reliable data base of aerodynamic coefficients and stability derivatives that would cover the Mach number and angle of attack range of interest to be used with the BSSM, SSM, DREV 6DOF trajectory programs and the CF-18 BIA OFP.

The lack of experimental data at Mach 1.5, in this case, was considered to be a deficiency as this would have allowed a better determination of the Mach number trend at Mach numbers higher than 1.1. It was initially planned to conduct test at this velocity regime, but this sabot design could not be used to launch the MPB-LD safely at this velocity (Ref. 8). An improved sabot design would be required to launch this type of projectiles at Mach 1.5, which is planned for future projects. Also, a redistribution of the test Mach numbers, for example 0.5, 0.9, 1.1 and 1.5, would provide the required test data to obtain the trends of the aerodynamic coefficients with Mach numbers so that the analytical tools could be used to their maximum efficiency.

8.0 CONCLUSIONS AND RECOMMENDATIONS

The aerodynamic characteristics of the Modular Practice Bomb - Low Drag (MPB-LD) or the BDU-5002/B MOD 1 were determined from free-flight tests conducted in the DREV aeroballistic range. Eleven projectiles were successfully fired in the Mach number range of 0.6 to 1.02. The aerodynamic coefficients and stability derivatives (C_{X0}, $C_{N\alpha}$, $C_{M\alpha}$, C_{Mq} and $C_{l\delta}\delta$) were well determined. The cubic pitch moment and the cubic normal force coefficient terms, the yaw axial force term, as well as induced moments and the trims were also reduced. Indraft wind tunnel, open jet facility experimental results, as well as full-scale tests were compared with the aeroballistic range results. Estimates of the aerodynamic coefficients from two analytical codes and from one computational fluid dynamic analyses were compared with the free-flight results.

The aerodynamic predictions from two empirical/analytical methodologies (PRODAS and AP95) as well as from a CFD analysis (Navier-Stokes) were evaluated. In general, the estimates provided for the MPB-LD computations were reasonable. There is not one individual code that could be used without reliable experimental data. The CFD analysis, limited to only static aerodynamic coefficients, did not provide more dependable estimates than the analytical predictions, but did provide good angle of attack data for the pitch moment coefficient.

On the other hand, and in many circumstances, even though the absolute values of the estimates were off the experimental data, the trends of the estimated aerodynamic coefficients with Mach numbers, when compared with the experimental data, were good. This seems to suggests that an astute combination of free-flight experimental data and the use of the analytical tools could provide a reliable data base of aerodynamic coefficients and stability derivatives that would cover the Mach number and angle of attack range of interest. The CFD analysis can provide nonlinear variations of some static coefficients with the angle of attack.

The lack of experimental data at Mach 1.5 was considered to be a deficiency as this would have allowed a better determination of the Mach number trend at Mach numbers higher than 1.1. A redistribution of the test Mach numbers, for example 0.5, 0.9, 1.1 and 1.5, would provide the required test data to obtain the trends of the aerodynamic coefficients with Mach numbers so that the analytical tools could be used to their maximum efficiency.

This data base of aerodynamic coefficients generated by this experimental program is considered a success and it can be used with the BSSM, the SSM, as well as the DREV 6DOF trajectory program to predict accurate weapon performance. Also, it can be exploited with confidence for the CF-18 OFP. The methodology should be extended to other weapon systems.

9.0 ACKNOWLEDGEMENTS

The author would like to thank Mrs. L. Audet for the operation of the aeroballistic range during the trials. Also, the perseverance of Mrs. S. Lafond, of SNC TEC, in developing, loading and reading the films with such thoroughness is appreciated and shown in the quality of the reduced coefficients. Thanks are also addressed to the whole CERM-V trials team for their devotion and to Mr. M. Normand, from MAETEC, for making these tests a success. The assistance of Mr. W. Hathaway in the data reductions was greatly appreciated.

10.0 REFERENCES

1. "ARFDAS97", Version 4.11, Arrow Tech Associates Inc, August 1997.

2. "Open Jet Facility Data Analysis System (OJFDAS)", Arrow Tech Associates Inc., DREV Contract No. W7701-0-1227, March 1992.

3. "Development of the MLM with Interference Coefficients and Tabular Aerodynamics for SSMDAS", Arrow Tech Associates, DREV contract No. W7701-5-2059, March 1996

4. Stathopoulos, N. and Ouellet, M., "Implementation of MLM for Store Separation Work - Phase II", Bombardier document MAU-261-213, May 1998

5. Jiang, L-J., "Advances in Aircraft/Store Separation Methodologies", NRC, LTR-A-001, October 1995

6. Drouin, G., Dupuis, A. and Côté, F., "Instrumentation Development and Data Analysis for the DREV Aeroballistic Range", DREV M-2800/87, March 1987, UNCLASSIFIED

7. Dupuis, A. and Drouin, G., "The DREV Aeroballistic Range and Data Analysis System", AIAA Paper No. 88-2017, AIAA 15th Aerodynamic Testing Conference, San Diego, California, 18-20 May, 1988.

8. Dupuis, A. D. and Normand, M., "Sabot Performance for Gun Launched MK82 CF, BDU-5003/B and BDU-5002/B MOD1 Bombs", DREV-TM-9734, January 1998, UNCLASSIFIED

9. Hathaway, W. H. and Whyte, R., "Aeroballistic Research Facility Free-Flight Data Analysis using the Maximum Likelihood function", AFATL-TR-79-98, December 1979, UNCLASSIFIED.

10. Whyte, R. and Hathaway, W., "Dynamic Calibration of Spark Aeroballistic Ranges", 44th Aeroballistic Range Association Meeting, 13-17 September., 1993, Munich.

11. "Projectile Design Analysis System (PRODAS), PC Version 3.9", Arrow Tech Associates Inc., 1995.

12. Girard, B., Drouin, G. and Cheers, B., "Supersonic Wind Tunnel Tests (MPBWT-5) of the Modular Practice Bomb", DREV M-2662/84, June 1984, UNCLASSIFIED

13. Girard, B., Cheers, B. and Lepage, R., "The Modular Practice Bomb as a Training Simulator for the BL-755 Cluster Bomb", DREV M-2740/85, August 1985, UNCLASSIFIED

14. Moore, F. G., McInville, R., M. and Hymer, T., "The 1995 Version of the NSWC Aeroprediction Code: Part I - Summary of New Theoretical Methodology", Naval Surface Weapons Center, NSWCCDD/TR-94/379, February 1995, UNCLASSIFIED

15. Bernier, A., "CFD Analysis of the MPB-LD Bomb", Contract number W7701-8-1480, 31 March 1999

16. Raw, M. J., Galpin, P. F. and Hutchinson, B. R., "A Co-located Finite Volume Method for Solving the Navier-Stokes Equations for Incompressible and Compressible Flows in Turbomachinery: Results and Applications", Canadian Aeronautics and Space Journal, Vol. 35, No. 4, 1989

TABLE I
Nominal physical properties of model

d (mm)	m (g)	I_x (g-cm^2)	I_y (g-cm^2)	l (mm)	CG from nose (% /100)
50.8	2715.1	9841.38	160465.1	432.816	0.46

TABLE II
Physical properties of test projectiles

Model #	d (mm)	l (mm)	CG from nose (mm)	CG from nose/l (-)	CG from nose (cal)	m (g)	I_x (g cm^2)	I_y (g cm^2)
B02	50.77	431.115	199.816	0.46349	3.94	2699.0	9777.29	159698.06
B03	51.18	431.471	200.248	0.46411	3.91	2758.9	10107.0	164149.97
B04	50.90	430.963	199.558	0.46305	3.92	2709.7	9821.27	159949.91
B05	50.98	432.106	201.063	0.46531	3.94	2730.8	9932.34	162169.39
B06	50.95	431.674	200.172	0.46371	3.93	2724.2	9884.59	160817.38
B08	50.90	431.572	200.411	0.46437	3.94	2725.7	9854.74	161772.36
B09	50.77	432.080	200.606	0.46428	3.95	2703.6	9773.66	159249.49
B10	50.77	431.293	199.671	0.46296	3.93	2697.9	9762.41	158997.12
B11	50.70	431.471	199.894	0.46329	3.94	2699.3	9762.77	159457.10
B12	50.81	431.852	200.504	0.46429	3.95	2705.4	9755.15	159375.76

TABLE III
Range conditions

Shot Number	No. of Stations	Observed Distance (m)	Pressure (mbar)	Temperature (degrees C)	Relative Humidity %	Air Density (kg/m3)	Speed of Sound (m/sec)	Reynolds Number
B981002	39	115.0	1001.17000	21.07	31.5000	1.1854	343.858	$.624 \times 10^7$
B981003	38	115.0	1000.00000	21.52	31.5000	1.1822	344.125	$.630 \times 10^7$
B981004	38	115.0	995.00000	21.13	36.0000	1.1779	343.896	$.710 \times 10^7$
B981005	38	115.0	995.30000	21.09	36.0000	1.1784	343.869	$.749 \times 10^7$
B981006	37	115.0	995.30000	21.30	36.0000	1.1776	343.994	$.782 \times 10^7$
B981008	38	115.0	987.14000	20.95	38.0000	1.1693	343.789	$.841 \times 10^7$
B981009	39	115.0	982.00000	21.01	39.0000	1.1629	343.827	$.890 \times 10^7$
B981010	24	62.2	987.60000	21.32	36.0000	1.1684	344.003	$.956 \times 10^7$
B981111	38	109.8	985.40000	20.72	33.0000	1.1681	343.656	$.972 \times 10^7$
B981112	41	169.7	985.00000	20.64	33.0000	1.1680	343.606	$.975 \times 10^7$

TABLE IV
Linear theory analysis parameters

Shot No.	Mach No.	Dbeq deg^2	KF deg	XS deg	LF 1/m	LS 1/m	WF deg/m	WS deg/m	WDF deg/m^2	WDS deg/m^2	KT deg	E-ANG deg
B981002	.645	10.50	4.97	4.25	-.0128	-.0115	14.00	-13.86	-.030	.026	.281	.368
B981003	.653	14.22	5.62	4.29	-.0115	-.0100	13.67	-13.95	-.025	.027	.128	.277
B981004	.739	26.35	6.63	6.13	-.0072	-.0145	15.43	-15.20	-.037	.026	.143	.754
B981005	.779	1.31	2.18	1.70	-.0245	-.0090	11.98	-11.70	-.004	-.001	.287	.203
B981006	.813	11.89	6.96	3.19	-.0154	-.0089	14.30	-15.67	-.031	.045	1.105	.688
B981008	.881	.87	1.52	1.11	-.0156	-.0081	11.97	-11.88	.000	.000	.413	.168
B981009	.937	.05	.87	.26	-.0351	-.0043	16.84	-9.81	-.157	.229	.214	.236
B981010	1.004	.36	.84	.68	-.0180	-.0200	14.00	-14.27	.000	.000	1.218	.339
B981111	1.020	.55	1.71	1.19	-.0184	-.0196	14.02	-13.98	.000	.000	.001	.168
B981112	1.022	.06	.46	.74	-.0179	-.0144	16.51	-8.64	-.031	-.092	.230	.272

UNCLASSIFIED

TABLE V
Linear theory aerodynamic coefficients

Shot No.	Mach No.	Dbeq deg^2	CX0	CX2	CNa	Cma	Cmq	Cnpa	Cld	Clp	Clpw	E-X m	E-SMR m	E-ANG deg	E-PHI deg
B981002	.645	10.5	.232	1.75	8.66	-12.13	-210.8	.01	-.0027	-4.0668	.0000	.0007	.0042	.368	.97
B981003	.653	14.2	.242	1.77	7.72	-12.49	-193.5	.01	-.0007	-4.0762	.0000	.0006	.0027	.277	1.26
B981004	.739	26.4	.228	1.99	9.04	-14.72	-184.5	.01	-.0060	-4.1835	.0000	.0014	.0020	.754	1.81
B981005	.779	1.3	.248	2.09	6.71	-11.30	-323.3	.01	-.0051	-4.2341	.0000	.0007	.0039	.203	.25
B981006	.813	11.9	.236	2.24	8.01	-13.33	-218.4	.01	.0064	-4.2863	.0000	.0009	.0013	.688	1.78
B981008	.881	.9	.266	2.73	7.74	-11.69	-215.9	.01	-.0030	-4.4228	.0000	.0006	.0006	.168	.39
B981009	.937	.1	.310	3.51	3.05	2.12	-400.1	.01	-.0046	-4.5412	.0000	.0006	.0018	.236	.47
B981010	1.004	.4	.506	4.36	14.13	-16.14	-332.3	.01	.0000	-4.6715	.0000	.0006	.0014	.339	.00
B981111	1.020	.6	.548	4.38	9.58	-15.89	-353.5	.01	.0000	-4.6778	.0000	.0005	.0008	.168	.00
B981112	1.022	.1	.552	4.38	23.90	-18.53	-228.8	.01	-.0025	-4.6788	.0000	.0006	.0012	.272	.51

UNCLASSIFIED

TABLE VI

Six-degree-of freedom aerodynamic coefficients - Single fits

Shot Number	Mach Number	DBSQ / ABARM	CX / CX2	CNa / CNa3	CYpa / Cnpa	Cma / Cma3	Cmq / Cmq2	CZga3 / Cnga3	CYga3 / Cnga3	Clga2 / Cnam	Clp / Cld	CNda / CNdB	Cmda / CmdB	Standard Error X(m) / Y-Z(m)	Standard Error Angle(deg) / Roll(deg)
B981002	.646	13.8	.241	7.84	.00	-10.279	-235.8	.0	.0	.00	-4.067	-.014	.055	.0007	.380
			(1.%)	(3.%)	(*)	(2.%)	(5.%)	(*)	(*)	(*)	(*)	(64.%)	(21.%)		
		9.0	1.0	59.0	.0	-364.8	.0	.0	-50.0	.00	-.003	-.017	-.017	.0010	1.524
			(*)	(*)	(*)	(9.%)	(*)	(*)	(*)	(*)	(5.%)	(48.%)	(84.%)		
B981003	.654	18.4	.246	8.07	.00	-10.381	-213.4	.0	.0	.00	-4.076	-.007	.039	.0006	.237
			(0.%)	(2.%)	(*)	(1.%)	(3.%)	(*)	(*)	(*)	(*)	(76.%)	(22.%)		
		9.4	1.0	59.0	.0	-317.9	.0	.0	-50.0	.00	-.001	.012	-.002	.0008	1.791
			(*)	(*)	(*)	(5.%)	(*)	(*)	(*)	(*)	(26.%)	(47.%)	(-)		
B981004	.740	30.5	.246	9.09	.00	-11.743	-185.1	.0	.0	.00	-4.183	.019	-.034	.0013	.673
			(4.%)	(4.%)	(*)	(4.%)	(8.%)	(*)	(*)	(*)	(*)	(96.%)	(81.%)		
		11 7	.1	59.0	.0	-230.1	.0	-31.7	-50.3	.00	-.006	-.045	-.062	.0018	2.598
			(-)	(*)	(*)	(14.%)	(*)	(43.%)	(12.%)	(*)	(4.%)	(36.%)	(43.%)		
B981005	.779	2.1	.248	8.30	.00	-11.441	-267.1	.0	.0	.00	-4.234	-.008	.023	.0006	.282
			(0.%)	(*)	(*)	(1.%)	(10.%)	(*)	(*)	(*)	(*)	(82.%)	(43.%)		
		3.3	1.0	59.0	.0	-250.0	.0	.0	-50.0	.00	-.005	-.015	-.052	.0008	.466
			(*)	(*)	(*)	(*)	(*)	(*)	(*)	(*)	(1.%)	(45.%)	(18.%)		
B981006	.814	17.2	.257	7.73	.00	-12.449	-285.9	.0	.0	.00	-4.286	.015	-.033	.0009	.670
			(1.%)	(5.%)	(*)	(3.%)	(8.%)	(*)	(*)	(*)	(*)	(*)	(-) (83.%)		
		8.5	1.0	.0	.0	-211.0	.0	.0	-100.0	.60	.006	-.156	-.247	.0020	5.454
			(*)	(*)	(*)	(17.%)	(*)	(*)	(*)	(*)	(8.%)	(12.%)	(12.%)		

UNCLASSIFIED

TABLE VI (continued)

Shot Number	Mach Number	DBSQ / ABAFN	CX / CX2	CMa / CMa3	CYpa / Cnpa	Cma / Cma3	Cmq / Cmq2	CNga3 / Cngq3	CYga3 / Cngq3	Clga2 / Cnam	Clp / Cld	CMda / CMdB	Cnda / CndB	Standard Error X(m) / Y-Z(m)	Standard Error Angle(deg) / Roll(deg)
B981008	.862	1.4	.266	7.77	.00	-11.692	-233.2	.0	.0	.00	-4.423	-.061	.085	.0006	.179
			(0.%)	(6.%)	(*)	(1.%)	(9.%)	(*)	(*)	(*)	(*)	(10.%)	(7.%)		
		2.4	2.7	.0	.0	-262.0		.0	.0	.00	-.003	.011	.001	.0005	.443
			(*)	(*)	(*)	(*)	(*)	(*)	(*)	(*)	(1.%)	(35.%)	(-)		
B981009	.937	.1	.310	8.00	.00	-12.924	-262.0	.0	.0	.00	-4.541	-.032	.026	.0006	.269
			(12.%)	(*)	(*)	(5.%)	(*)	(*)	(*)	(*)	(*)	(19.%)	(38.%)		
		.7	3.5	.0	.0	-260.0		.0	.0	.00	-.005	.033	.045	.0016	.549
			(*)	(*)	(*)	(*)	(*)	(*)	(*)	(*)	(1.%)	(18.%)	(23.%)		
B981010	1.004	2.0	.511	8.30	.00	-14.368	-350.0	.0	.0	.00	-4.672	-.008	-.028	.0007	.320
			(2.%)	(*)	(*)	(5.%)	(*)	(*)	(*)	(*)	(*)	(-)	(61.%)		
		2.2	4.4	.0	.0	.0	.0	.0	.0	.00	.000	-.164	-.301	.0009	.000
			(*)	(*)	(*)	(*)	(*)	(*)	(*)	(*)	(*)	(6.%)	(7.%)		
B981111	1.020	1.0	.549	8.57	.00	-16.102	-358.0	.0	.0	.00	-4.678	-.005	.017	.0006	.111
			(0.%)	(6.%)	(*)	(1.%)	(4.%)	(*)	(*)	(*)	(*)	(82.%)	(42.%)		
		2.8	4.4	.0	.0	.0	.0	.0	.0	.00	.001	-.024	-.045	.0003	.000
			(*)	(*)	(*)	(*)	(*)	(*)	(*)	(*)	(-)	(13.%)	(12.%)		
B981112	1.023	.1	.554	8.30	.00	-14.897	-350.0	.0	.0	.00	-4.679	.010	-.016	.0007	.334
			(1.%)	(*)	(*)	(5.%)	(*)	(*)	(*)	(*)	(*)	(69.%)	(84.%)		
		.9	4.4	.0	.0	.0	.0	.0	.0	.00	-.002	-.025	-.055	.0010	.698
			(*)	(*)	(*)	(*)	(*)	(*)	(*)	(*)	(1.%)	(28.%)	(25.%)		

UNCLASSIFIED

TABLE VII

Six-degree-of freedom aerodynamic coefficients - Multiple fits

Shot Numbers		Mach Number	DBSQ ABARM	CX CX2 CX4	CNa CNa3 CNa5	CYps Cnps Cnpa3	Cma Cma3 Cma5	Cmq Cmq2 Cmq4	Clga3 Cngs3 Cngs	CYga3 Cngs3 Cngs5	Clga2 CYga2 Clp	CXN CmaN CnaN	Standard Error X(m) Y-Z(m)	 Angle(deg) Roll(deg)
B981002	B981003	.705	16.2	.245 (1.%) .0 (*)	8.31 (3.%) .0 (*)	.00 (*) .0 (*)	-10.964 (1.%) .0 (*)	-208.7 (3.%) .0 (*)	.0 (*) .0 (*)	.0 (*) .0 (*)	.00 (*) -6.23 (*)	.04 (*) (30.%) .00 (*)	.0010	.451
B981004	B981005		11.9	.8 (33.%) .0 (*)	57.1 (26.%) .0 (*)	.0 (*) .0 (*)	-276.7 (4.%) .0 (*)	.0 (*) .0 (*)	.0 (*) (7.%) .0 (*)	-49.9 (*) .0 (*)	.00 (*) -6.23 (*)	.00 (*) .00 (*)	.0012	1.703
B981005	B981006	.853	5.3	.247 (0.%) 1.0 (*)	7.96 (3.%) .0 (*)	.00 (*) .0 (*)	-11.801 (1.%) .0 (*)	-262.0 (4.%) .0 (*)	.0 (*) .0 (*)	.0 (*) .0 (*)	.00 (*) -6.54 (*)	-.01 (-) .00 (*)	.0009	.390
B981008	B981009		8.4	1.0 (*) .0 (*)	.0 (*) .0 (*)	.0 (*) .0 (*)	-260.2 (6.%) .0 (*)	.0 (*) .0 (*)	.0 (*) (12.%) .0 (*)	-124.7 (*) .0 (*)	.00 (*) -6.54 (*)	.00 (*) .00 (*)	.0014	2.973
B981010	B981111	1.016	1.0	.542 (0.%) 1.0 (*)	8.35 (9.%) .0 (*)	.00 (*) .0 (*)	-15.680 (1.%) .0 (*)	-354.2 (9.%) .0 (*)	.0 (*) .0 (*)	.0 (*) .0 (*)	.00 (*) -4.68 (*)	1.74 (*) (5.%) .00 (*)	.0008	.270
B981112			2.7	1.0 (*) .0 (*)	.0 (*) .0 (*)	.0 (*) .0 (*)	-250.0 (*) .0 (*)	.0 (*) .0 (*)	.0 (*) .0 (*)	.0 (*) .0 (*)	.00 (*) -4.68 (*)	.00 (*) .00 (*)	.0008	.435

UNCLASSIFIED

TABLE VIII
Experimental results

a) Full scale free-flight (Ref. 13)

Mach	C_D
0.60	0.27
0.74	0.28
0.79	0.29
0.83	0.29
0.86	0.30
0.88	0.31
0.89	0.31
0.90	0.32
0.91	0.34
0.94	0.43

b) DREV Indraft Wind Tunnel (Ref. 12)

Mach	C_{X0}	$C_{N\alpha}$	$C_{M\alpha}$
0.5	0.229	7.16	-11.06
0.6	0.225	7.62	-12.41
0.7	0.233	7.96	-13.17
0.8	0.242	8.31	-13.87
0.9	0.282	8.37	-13.82
1.5	0.729	7.96	-11.05

c) DREV Open Jet Facility (Ref. 2)

Mach	C_{X0}	$C_{N\alpha}$	$C_{M\alpha}$
0.877	0.364	8.08	-11.20

TABLE IX
CFD estimated aerodynamic coefficients

Mach	C_{X0}	$C_{N\alpha}$	$C_{N_{\alpha^3}}$	$C_{M\alpha}$	$C_{M_{\alpha^3}}$
0.5	0.337	8.72	37.96	-14.15	-106.42
0.8	0.377	9.31	35.09	-16.15	-78.88
0.9	0.415	9.01	57.44	-15.22	-146.48
1.1	0.654	10.42	34.29	-19.57	-57.66
1.5	0.631	8.96	31.34	-14.43	-30.01

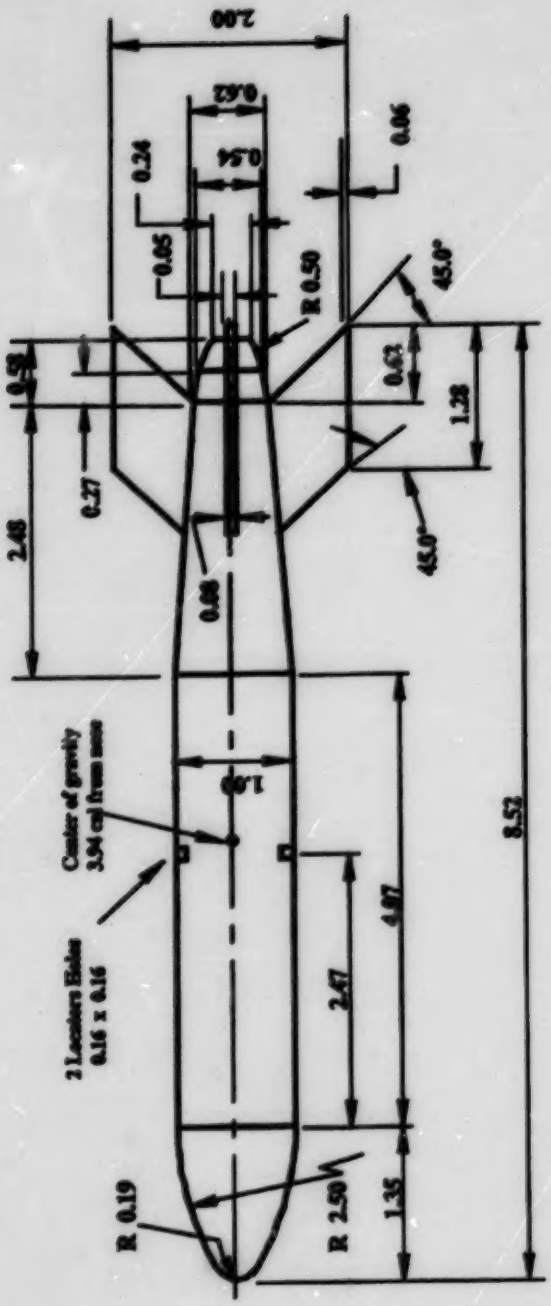

FIGURE 1 - MPB-LD geometry for aeroballistic range tests
(all dimensions in caliber, 1 cal = 50.8 mm)

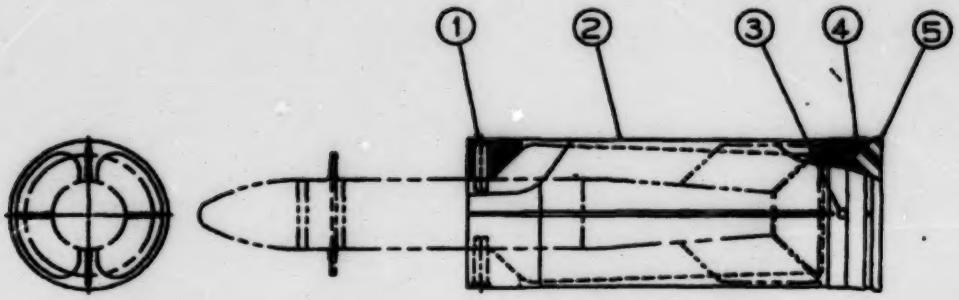

FIGURE 2 - Sabot schematic for the MPB-LD projectile

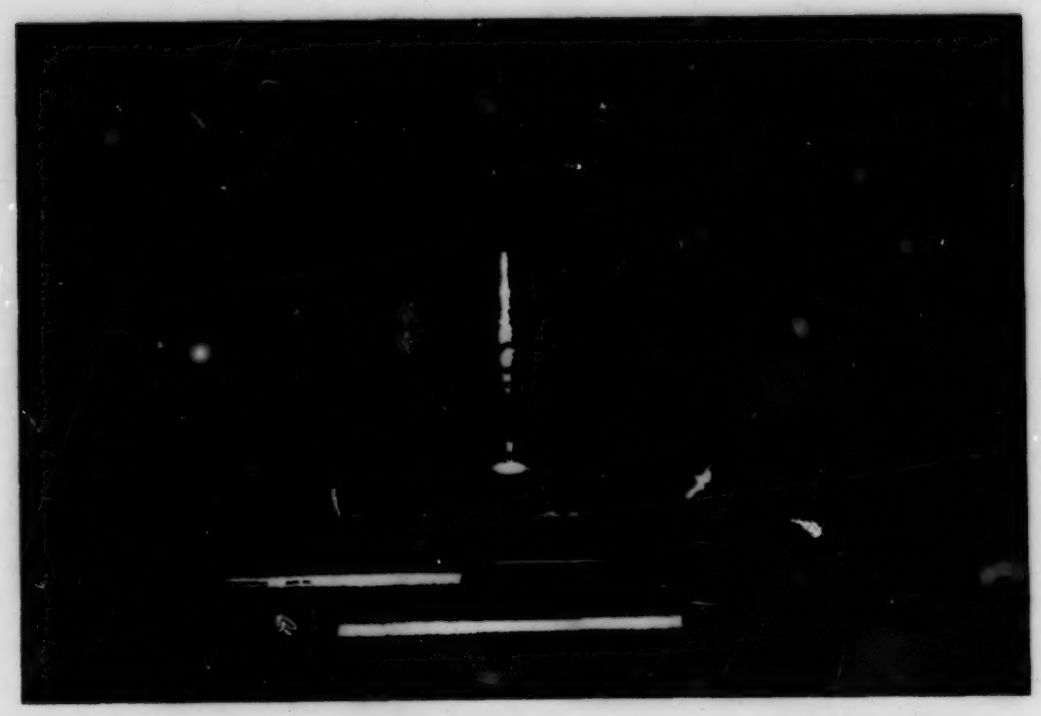

FIGURE 3 - Photograph of model and sabot package for the MPB-LD bomb

FIGURE 4 - DREV aeroballistic range

Fig. 4a) Photograph of aeroballistic range complex

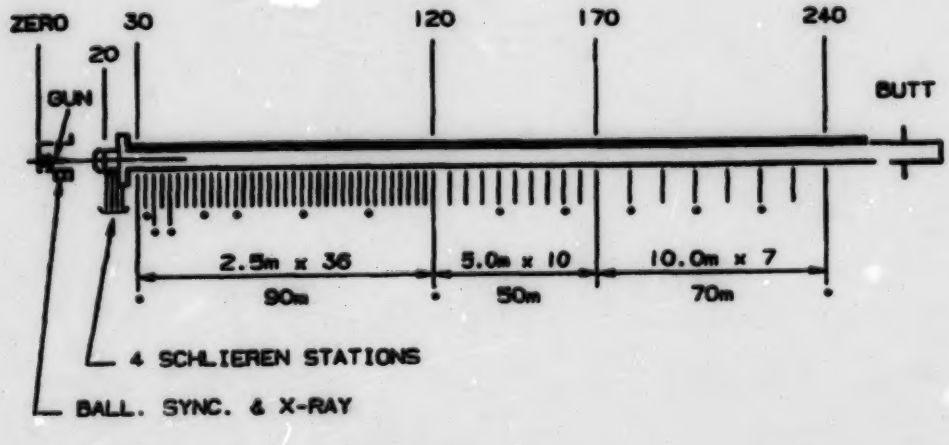

Fig. 4b) Photographic station spacing

FIGURE 5 - Typical Schlieren photograph for MPB-LD - Shot B09

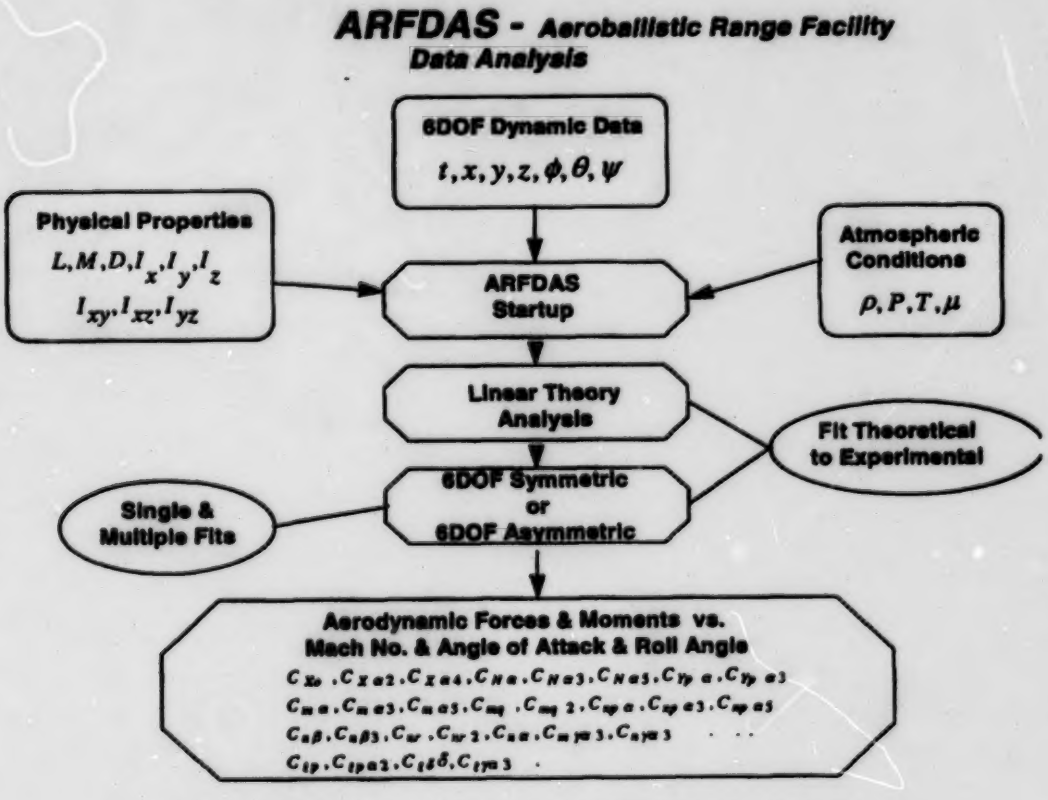
ARFDAS - Aeroballistic Range Facility
Data Analysis
6DOF Dynamic Data
t, x, y, z, φ, θ, ψ
Physical Properties
L, M, D, I_x, I_y, I_z
I_xy, I_xz, I_yz
Atmospheric Conditions
ρ, P, T, μ
ARFDAS
Startup
Linear Theory
Analysis
Fit Theoretical
to Experimental
6DOF Symmetric
or
6DOF Asymmetric
Single &
Multiple Fits
Aerodynamic Forces & Moments vs.
Mach No. & Angle of Attack & Roll Angle
C_Xo, C_Xα2, C_Xα4, C_Nα, C_Nα3, C_Nα5, C_Yp α, C_Yp α3
C_lα, C_lα3, C_lα5, C_lq, C_lq2, C_lp α, C_lp α3, C_lp α5
C_aβ, C_aβ3, C_lr, C_lr2, C_lα α, C_lr yα3, C_ayα3 . . .
C_lp, C_lpα2, C_lδδ, C_lyα3 .

FIGURE 6 - DREV Aeroballistic Range Facility Data Analysis System

FIGURE 7 – Comparison of 6DOF reduced aerodynamic coefficients versus Mach number

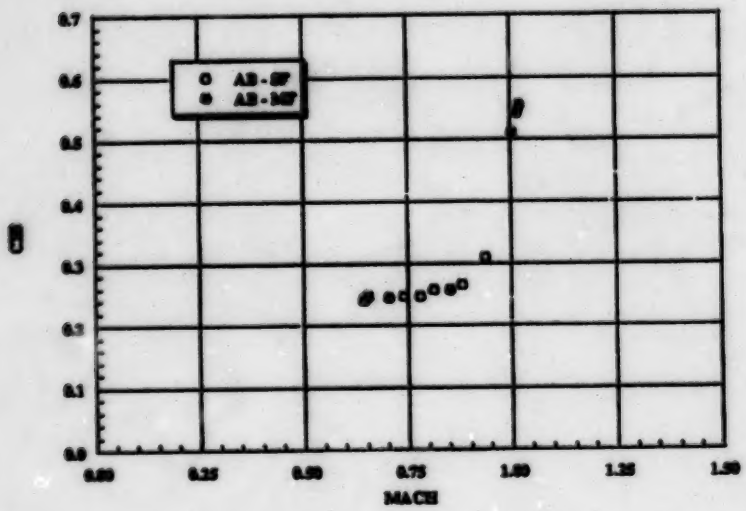

Fig. 7a) Axial force coefficient

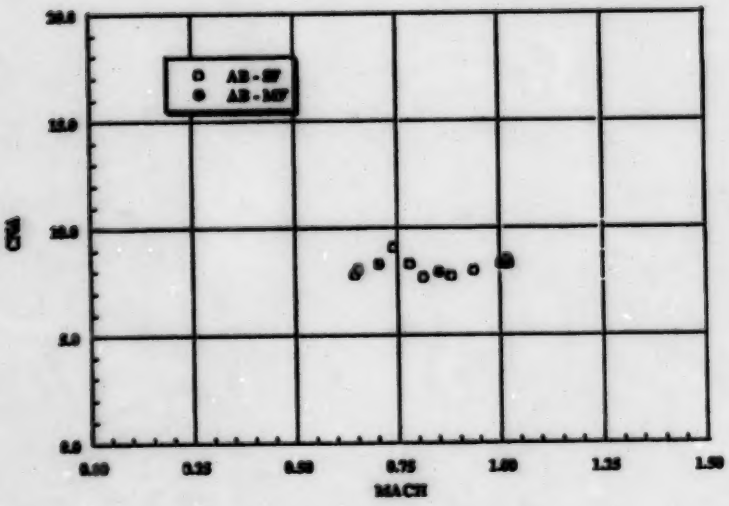

Fig. 7b) Normal force coefficient slope

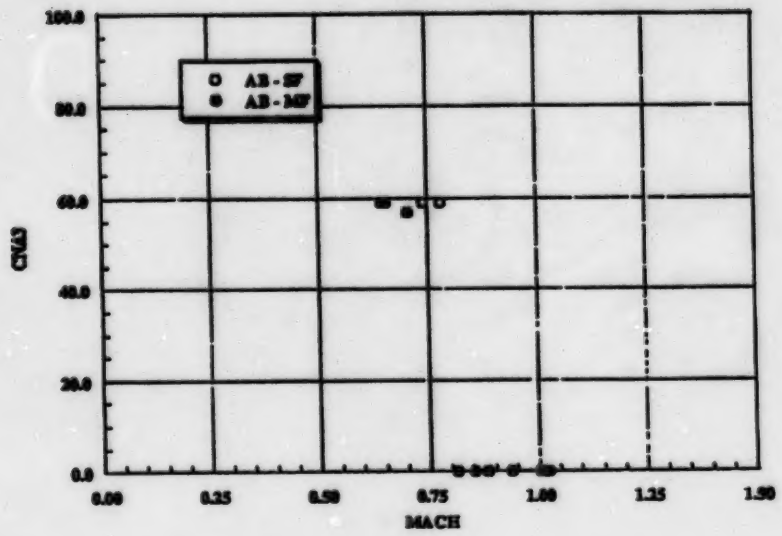

Fig. 7c) Cubic normal force coefficient term

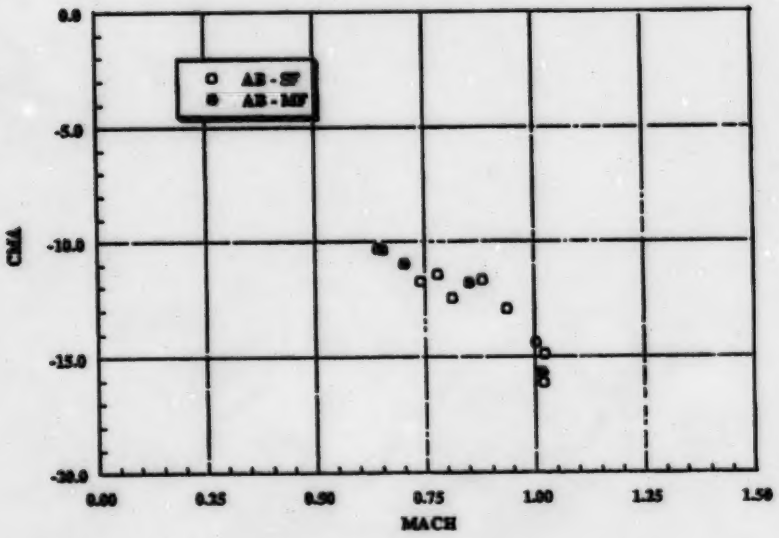

Fig. 7d) Pitch moment coefficient slope

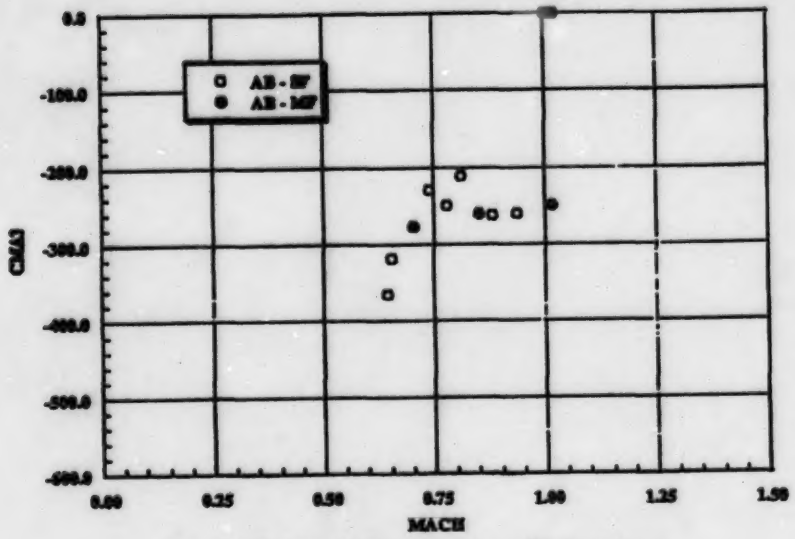

Fig. 7e) Cubic pitch moment coefficient term

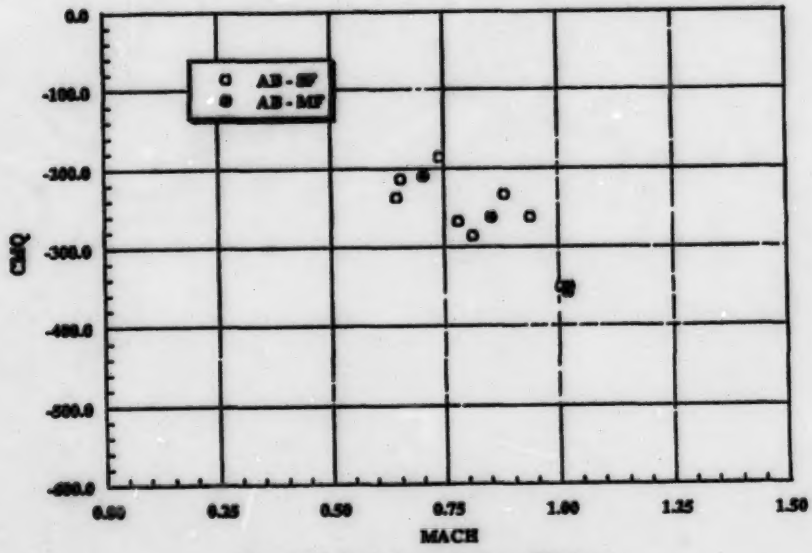

Fig. 7f) Pitch damping coefficient

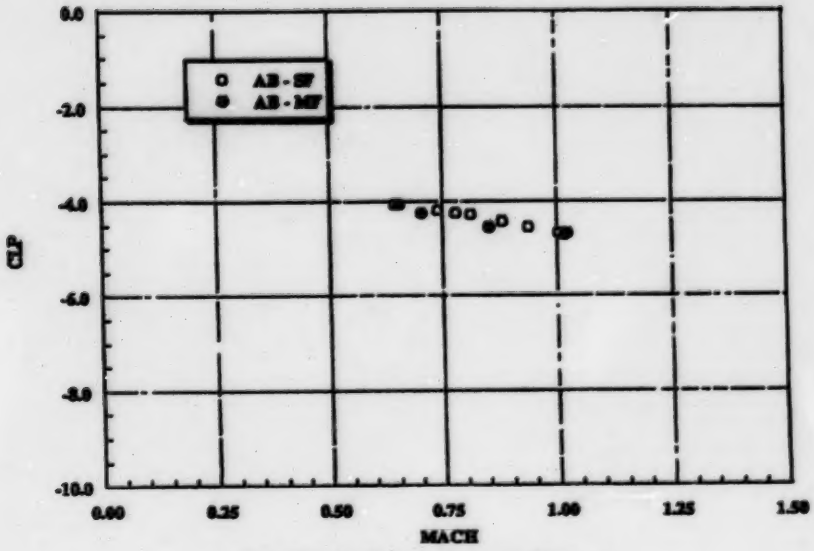

Fig. 7g) Roll damping coefficient

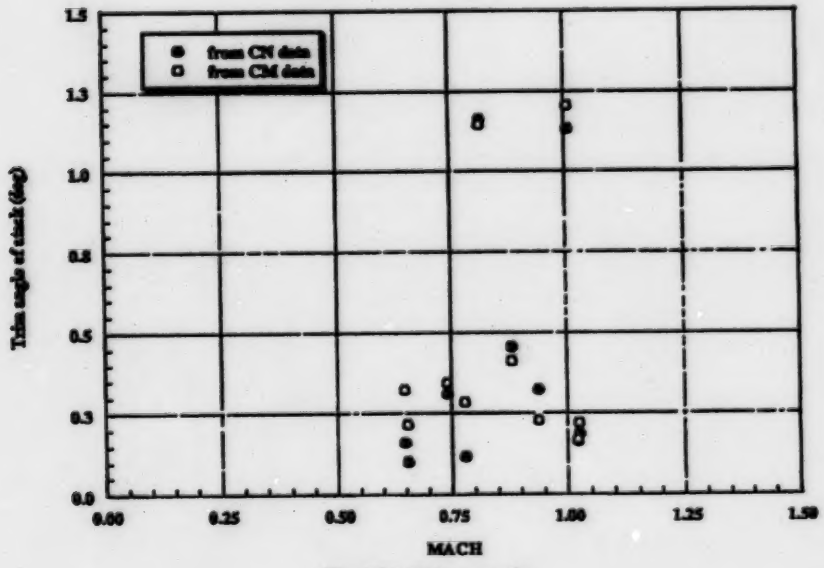

Fig 7h) Trim angle

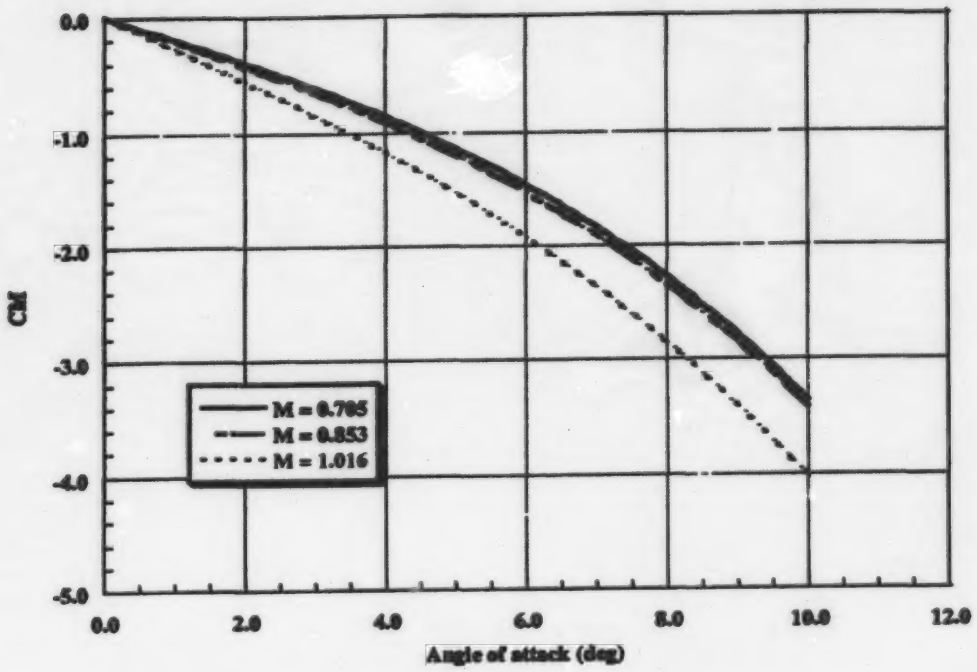

FIGURE 8 – Pitch moment coefficient versus angle of attack

FIGURE 9 – Comparison of experimental results versus Mach number

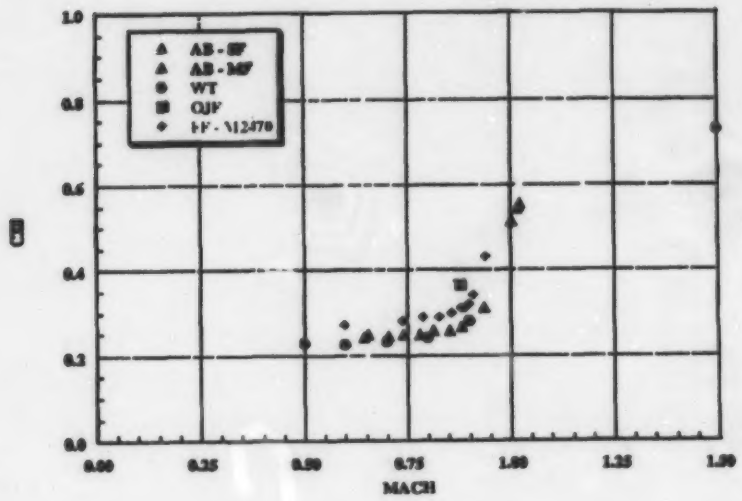

Fig. 9a) Axial force coefficient

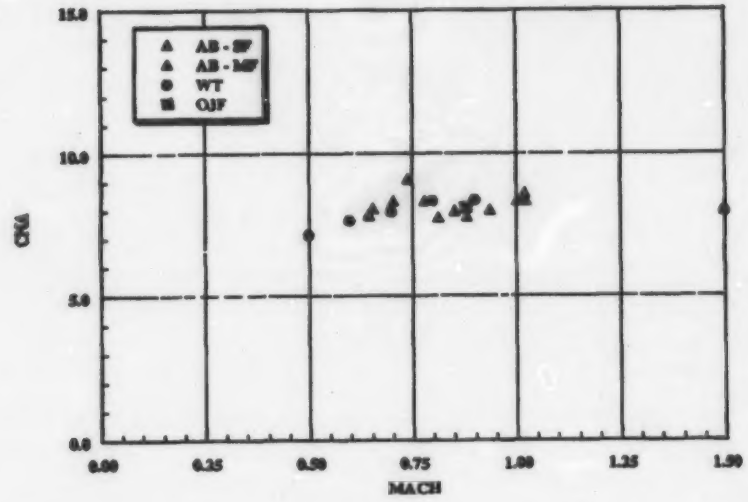

Fig. 9b) Normal force coefficient slope

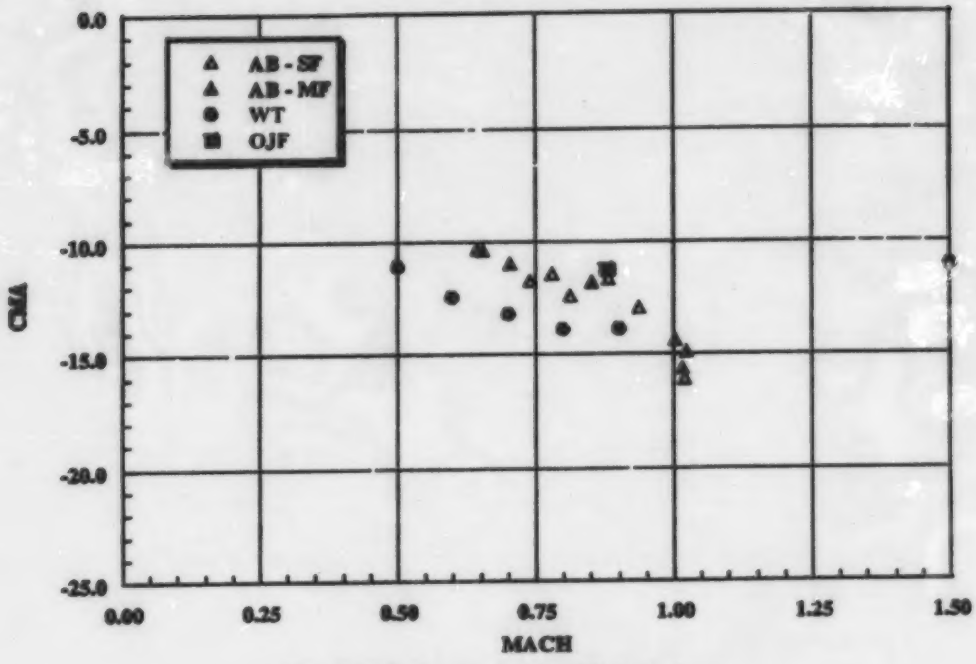

Fig. 9c) Pitch moment coefficient slope

FIGURE 10 – Comparison of predicted and experimental results

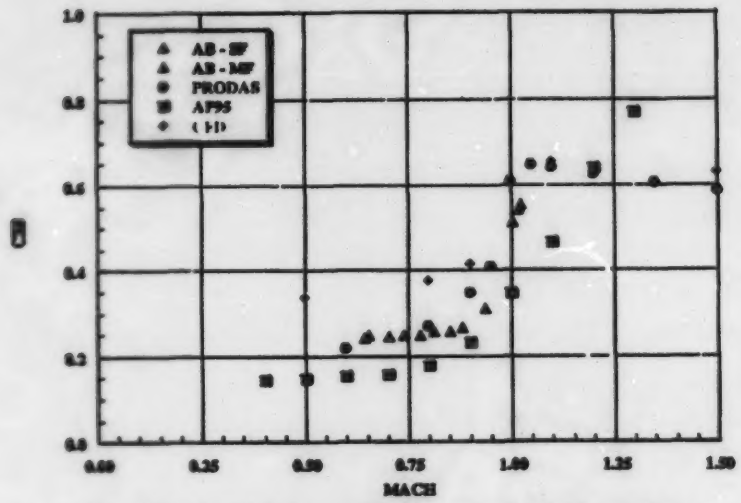

Fig. 10a) Axial force coefficient versus Mach number

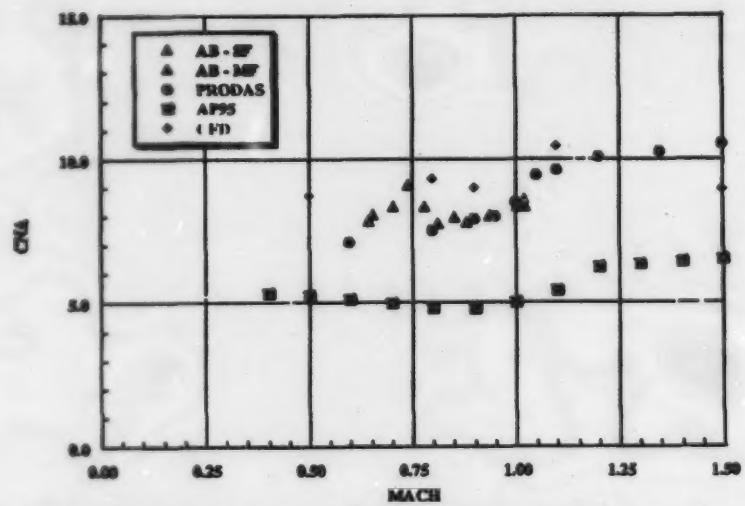

Fig. 10b) Normal force coefficient slope versus Mach number

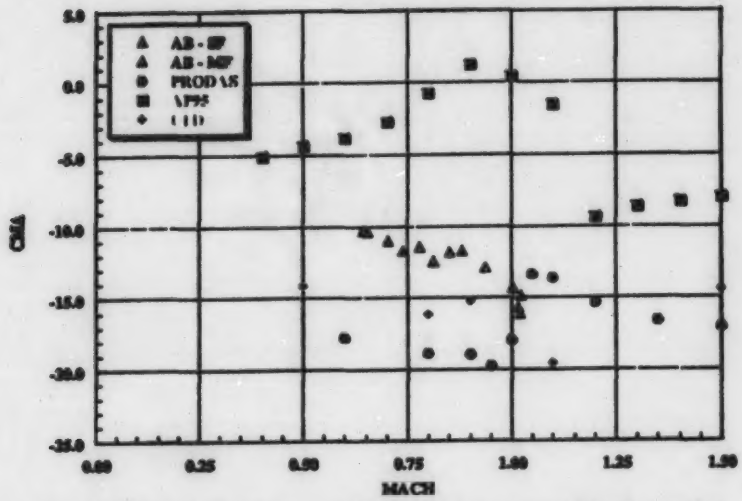

Fig. 10c) Pitch moment coefficient slope versus Mach number

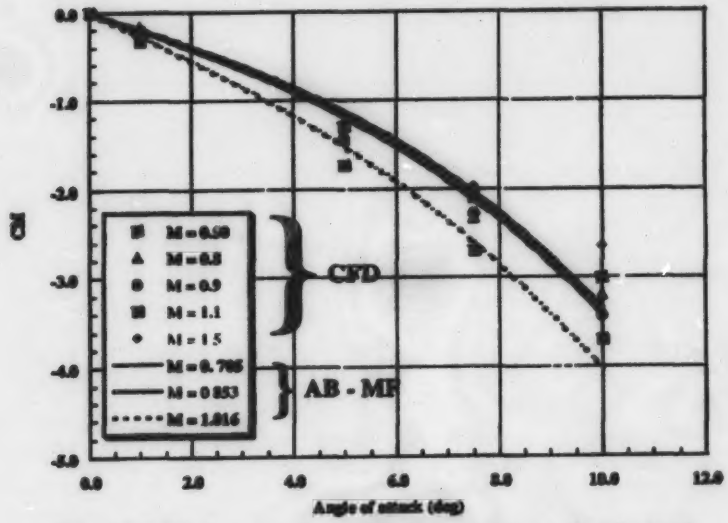

Fig. 10d) Pitch moment coefficient versus angle of attack

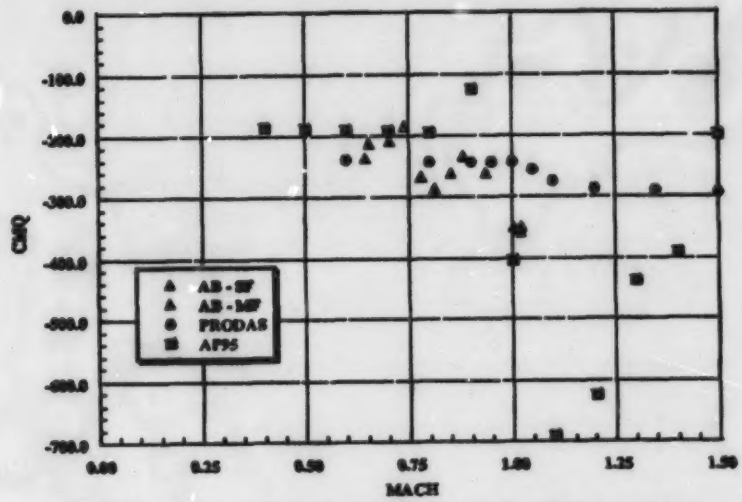

Fig. 10e) Pitch damping coefficient versus Mach number

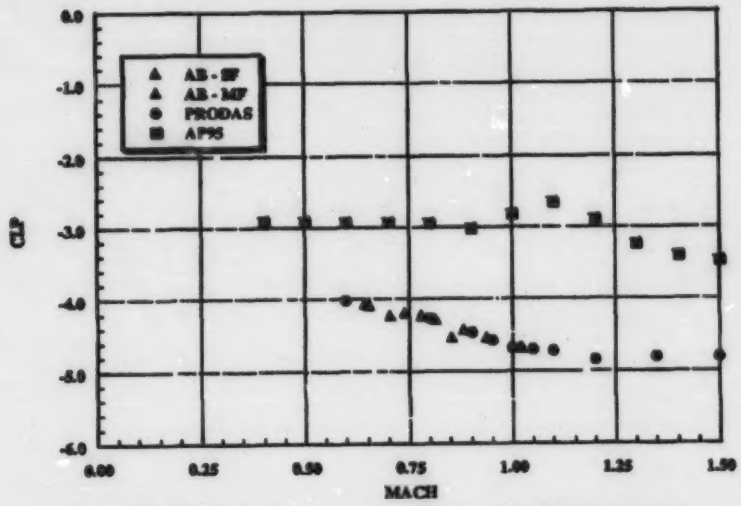

Fig. 10f) Roll damping coefficient versus Mach number

APPENDIX A

Angular Motion Plots

B981002

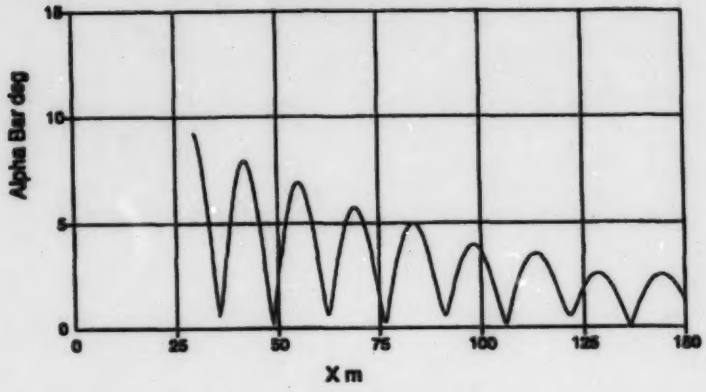

B981002

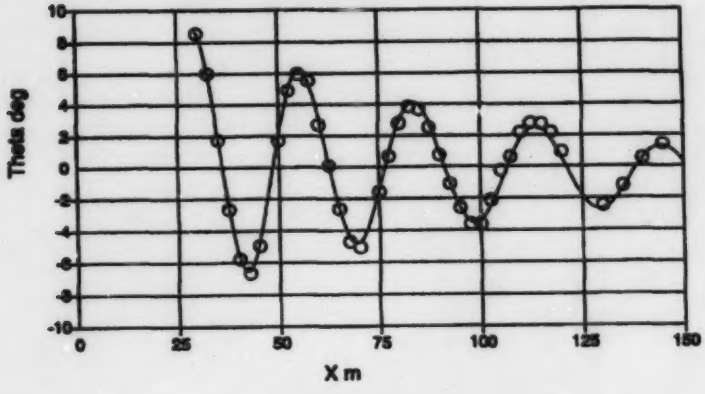

B981002

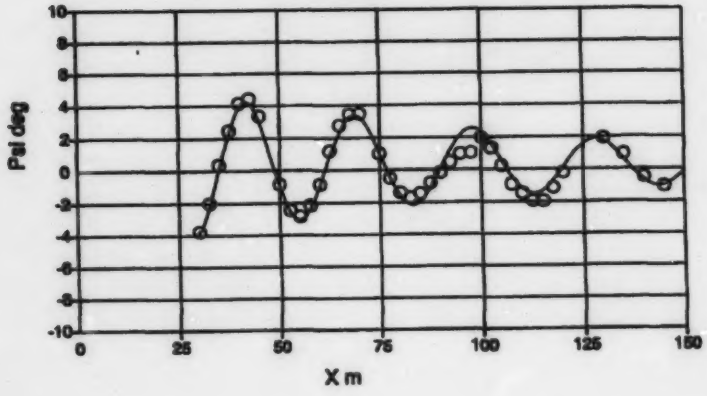

B981003

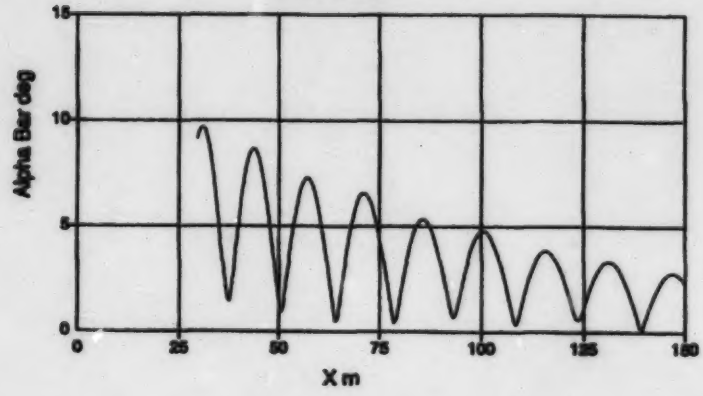

B981003

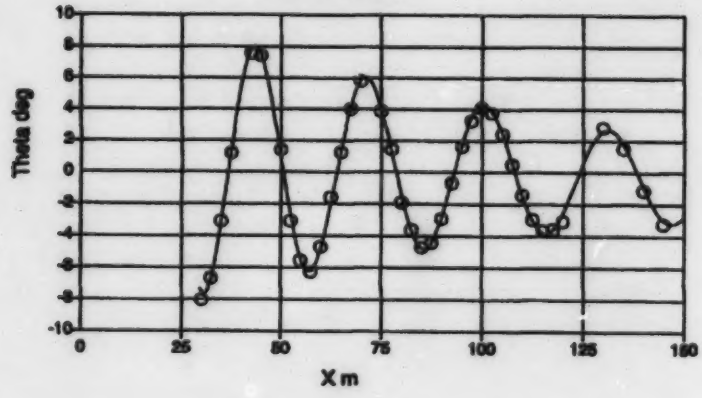

B981003

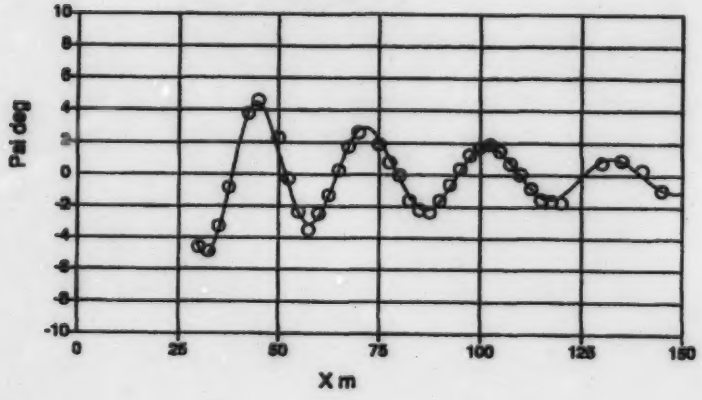

B981004

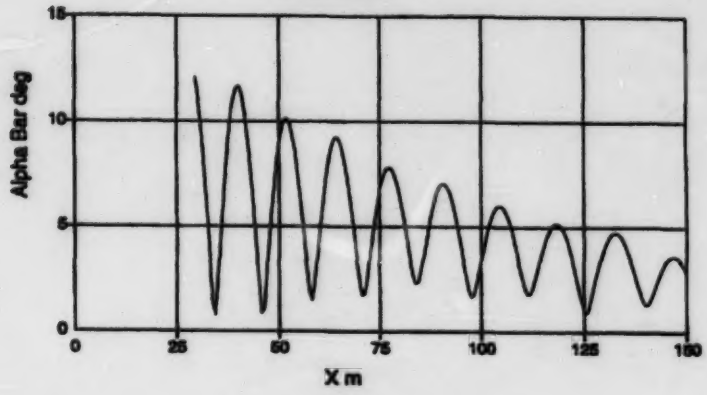

B981004

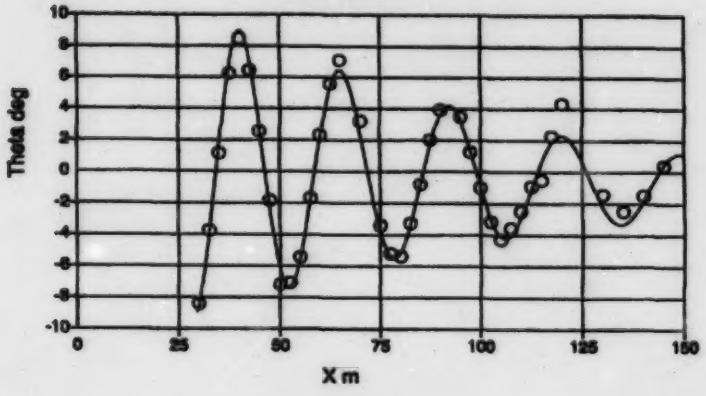

B981004

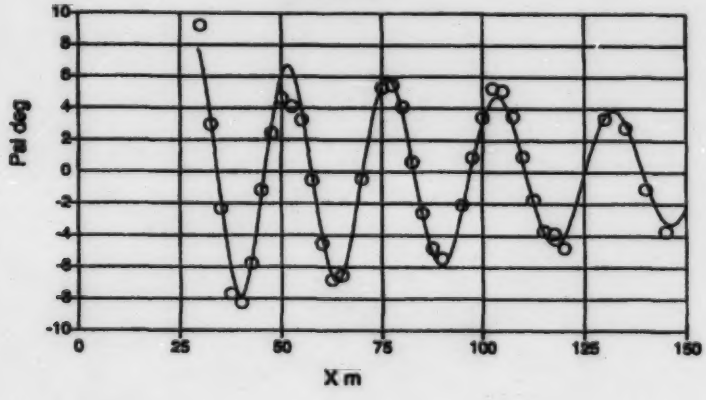

B981005

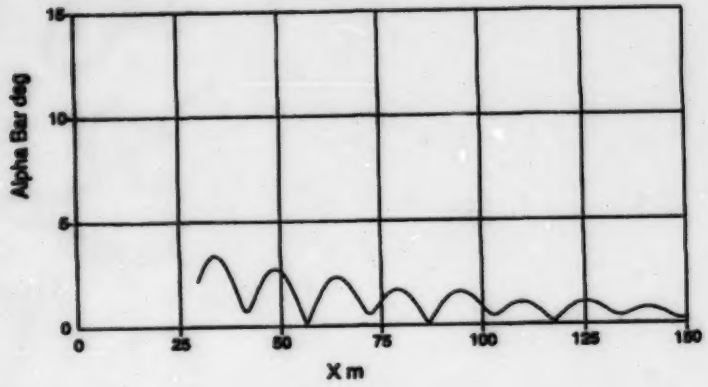

B981005

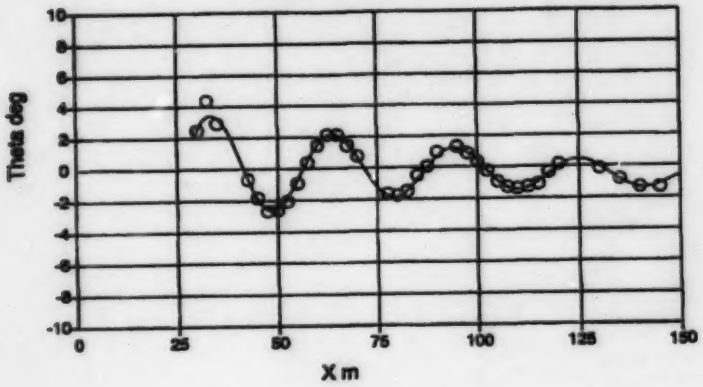

B981005

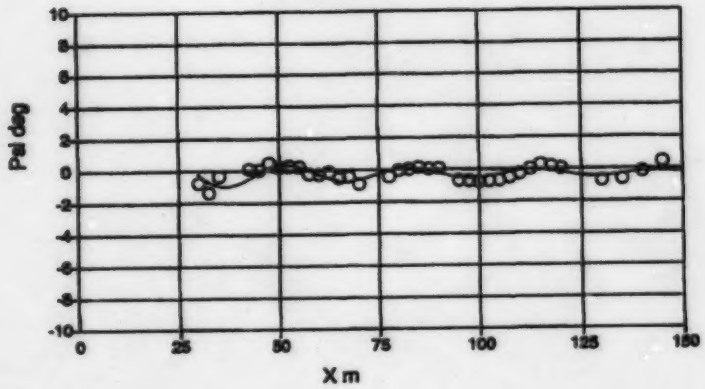

B981006

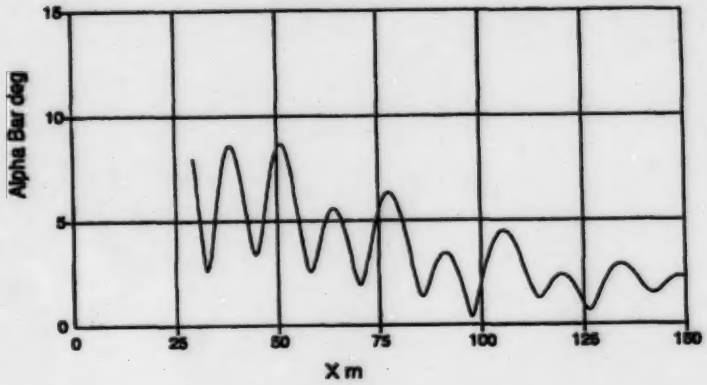

B981006

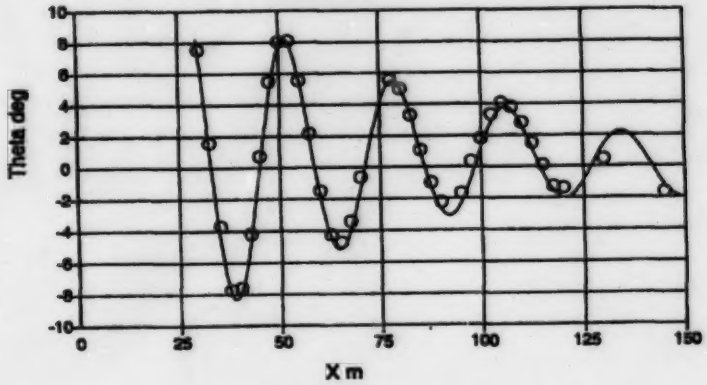

B981006

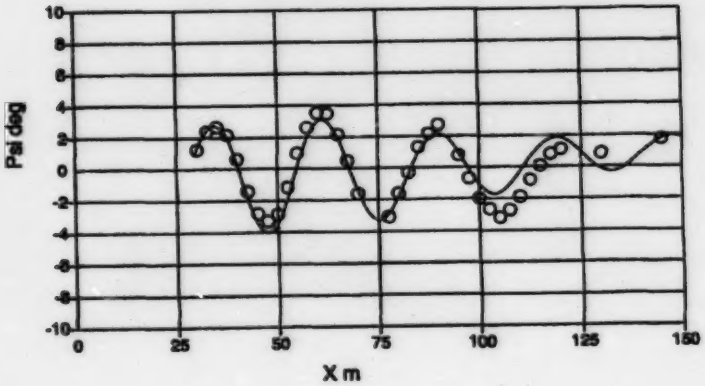

B981008

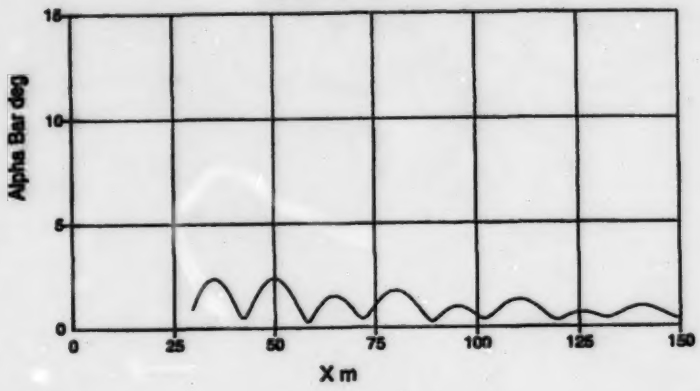

B981008

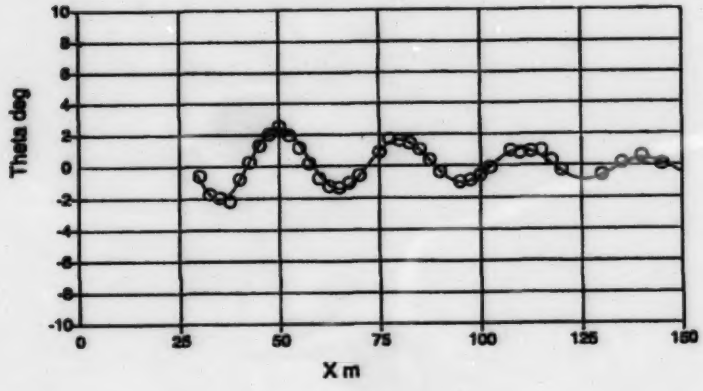

B981008

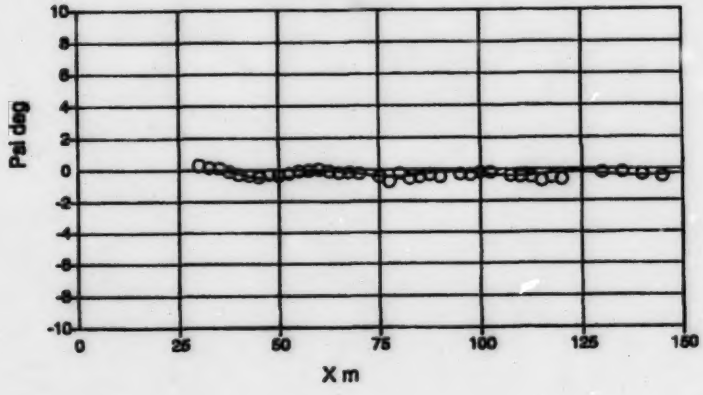

B981009

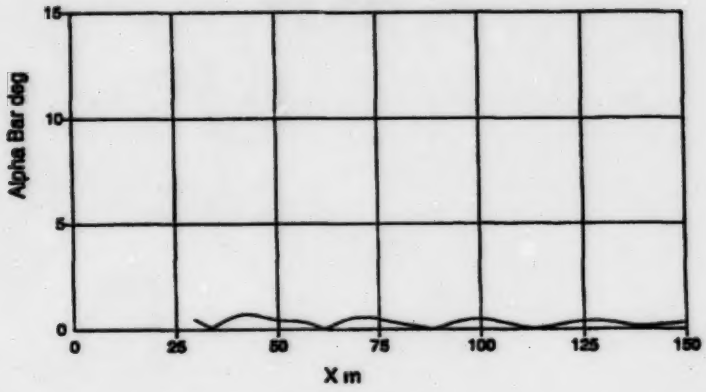

B981009

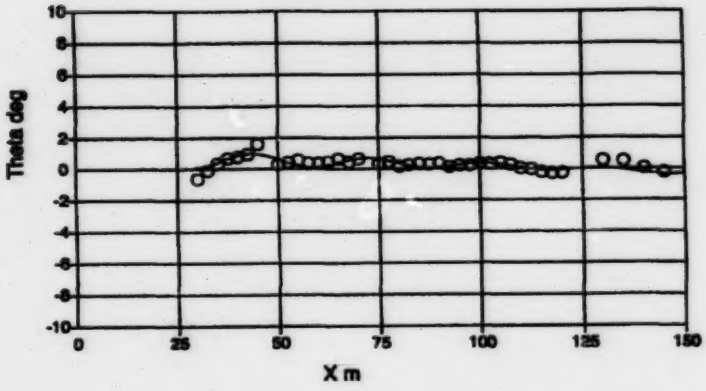

B981009

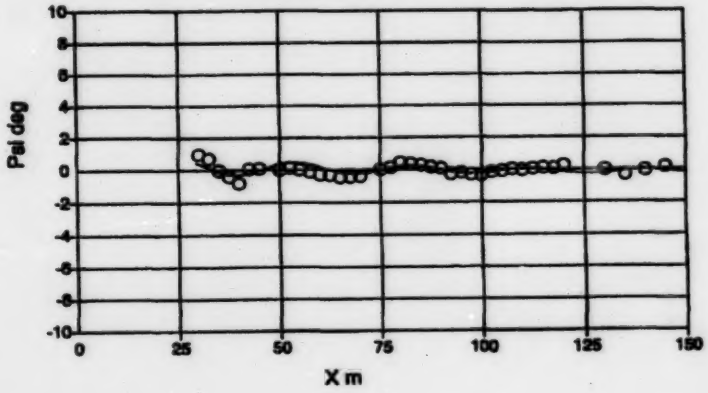

B981010

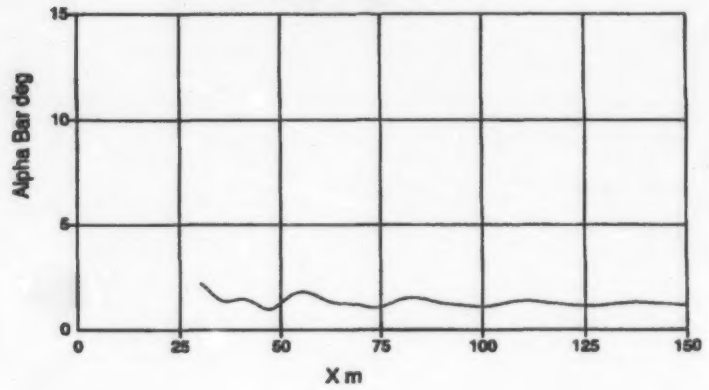

B981010

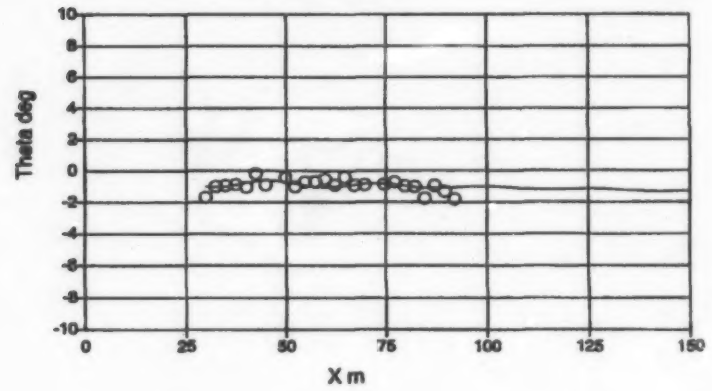

B981010

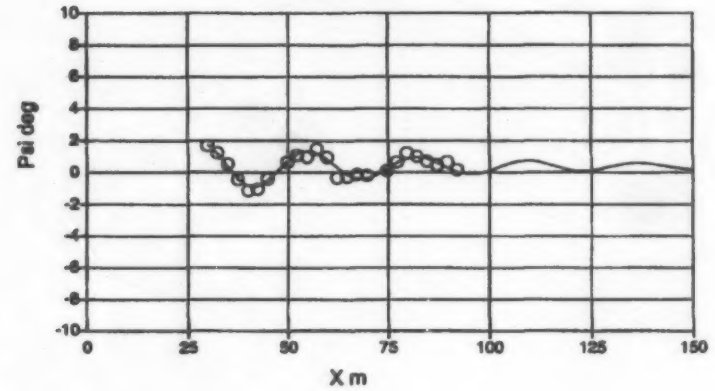

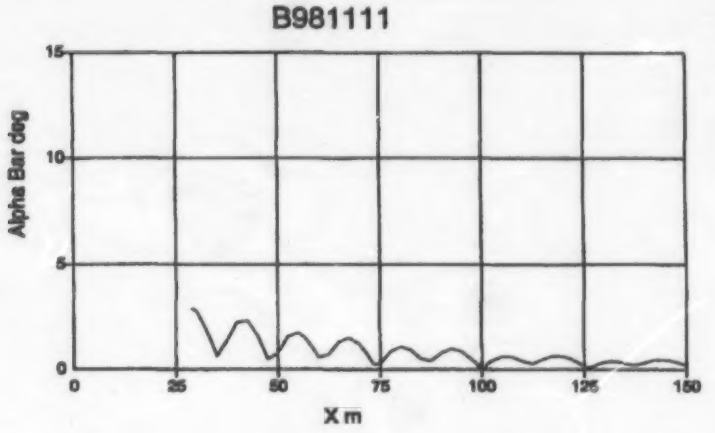

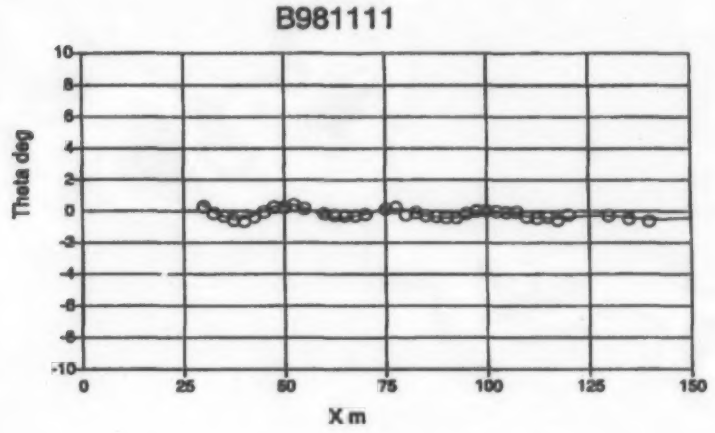

Figure 1 Theta vs X

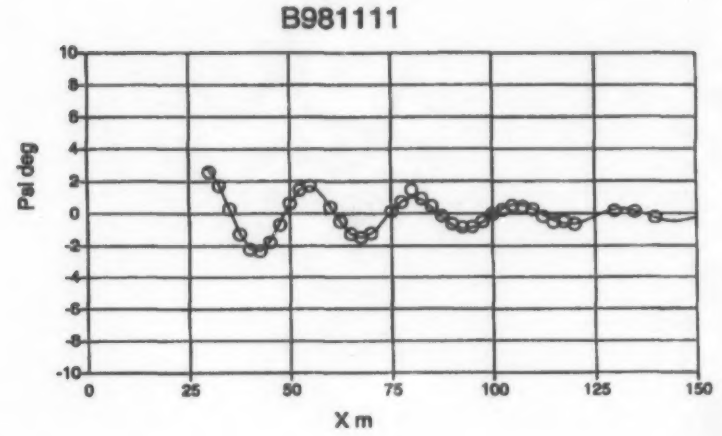

B981112

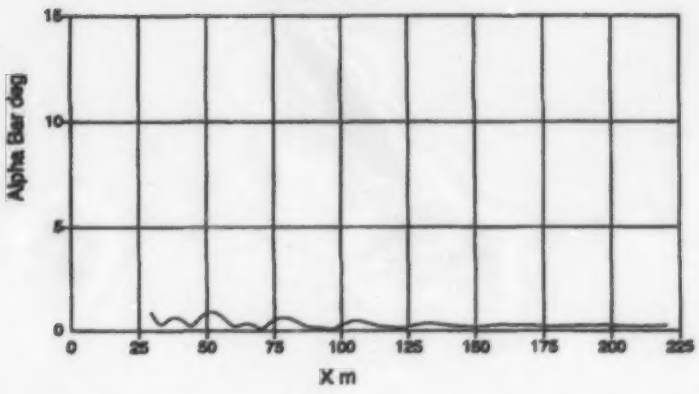

B981112

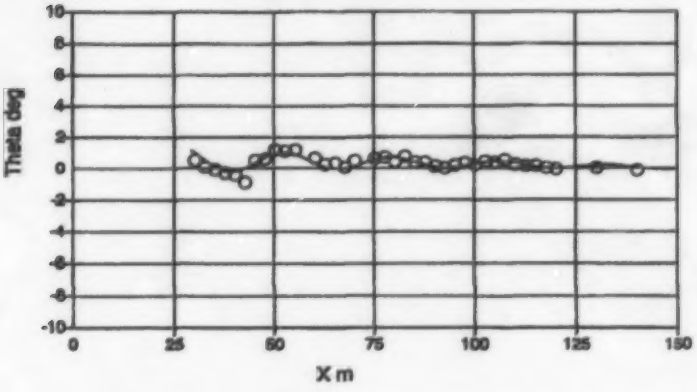

B981112

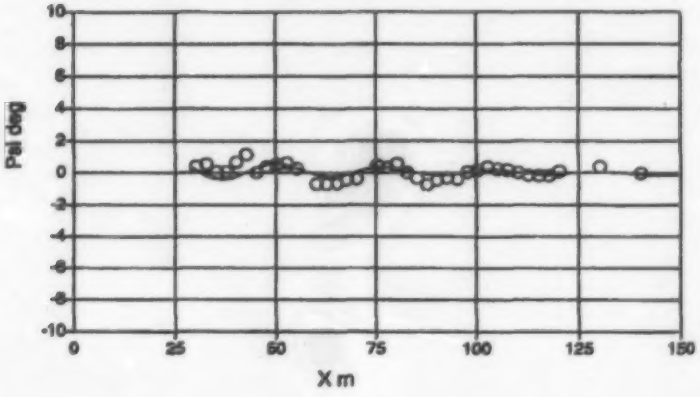

APPENDIX B

CFD Results

TABLE B1
CFD Results

Angle of attack (deg)	C_X	C_N	C_M
0.0°	0.337	-	-
1.0°	0.308	0.143	-0.221
5.0°	0.309	0.782	-1.295
7.5°	0.308	1.228	-2.102
10.0°	0.307	1.710	-3.008

Table B1 a) Mach = 0.5

Angle of attack (deg)	C_X	C_N	C_M
0.0°	0.377	-	-
1.0°	0.362	0.099	-0.160
5.0°	0.381	0.846	-1.448
7.5°	0.377	1.299	-2.335
10.0°	0.385	1.796	-3.198

Table B1 b) Mach = 0.8

Angle of attack (deg)	C_X	C_N	C_M
0.0°	0.415	-	-
1.0°	0.434	0.192	-0.328
5.0°	0.432	0.826	-1.440
7.5°	0.423	1.289	-2.275
10.0°	0.431	1.870	-3.424

Table B1 c) Mach = 0.9

Angle of attack (deg)	C_X	C_N	C_M
0.0°	0.654	-	-
1.0°	0.640	0.177	-0.330
5.0°	0.665	0.932	-1.741
7.5°	0.671	1.437	-2.690
10.0°	0.680	1.989	-3.698

Table B1 d) Mach = 1.1

Angle of attack (deg)	C_X	C_N	C_M
0.0°	0.631	-	-
1.0°	0.634	0.146	-0.215
5.0°	0.643	0.799	-1.267
7.5°	0.651	1.246	-1.973
10.0°	0.659	1.718	-2.654

Table B1 e) Mach = 1.5

FIGURE B1 – CFD results

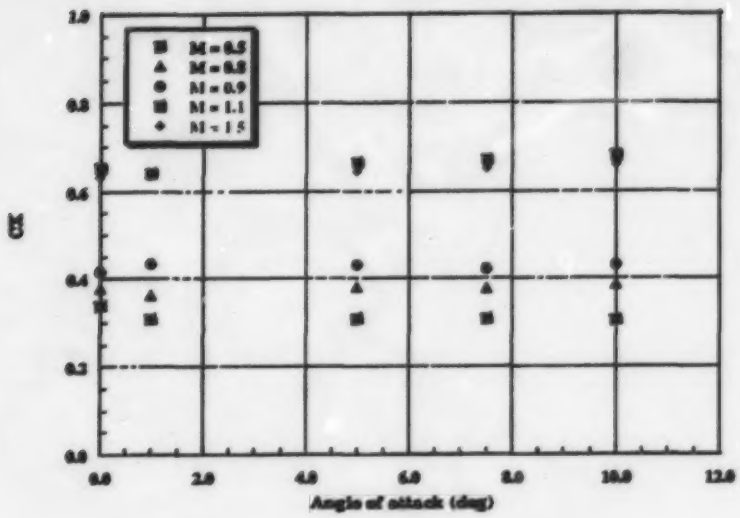

Fig. B1 a) Axial force coefficient

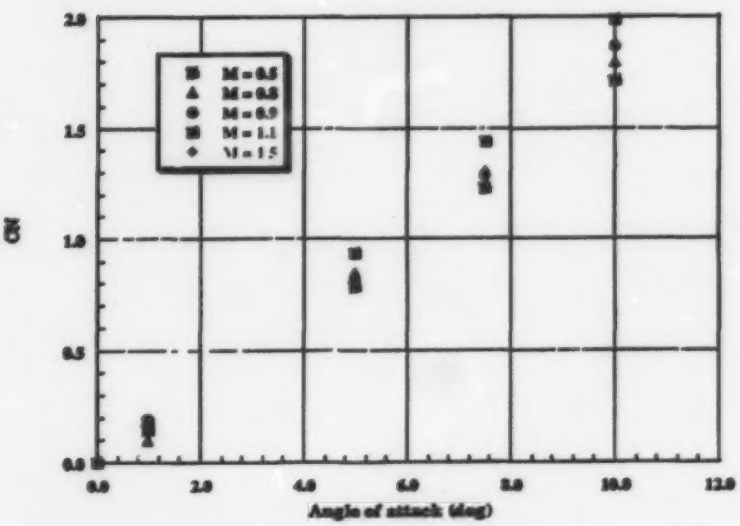

Fig. B1 b) Normal force coefficient

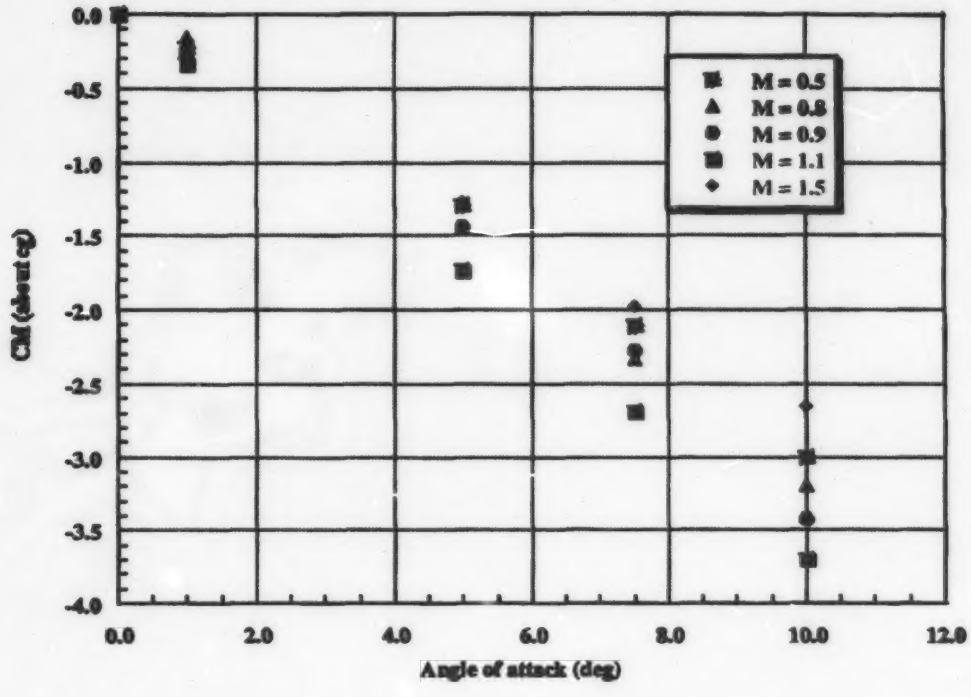

Fig. B1 c) Pitch moment coefficient

APPENDIX C

Comparison of All Results

FIGURE C1 – Comparison of all aerodynamic coefficients results versus Mach number

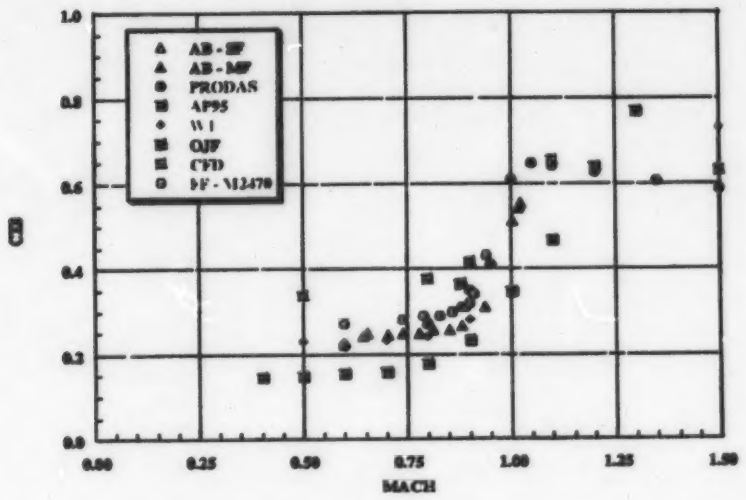

Fig. C1 a) Axial force coefficient

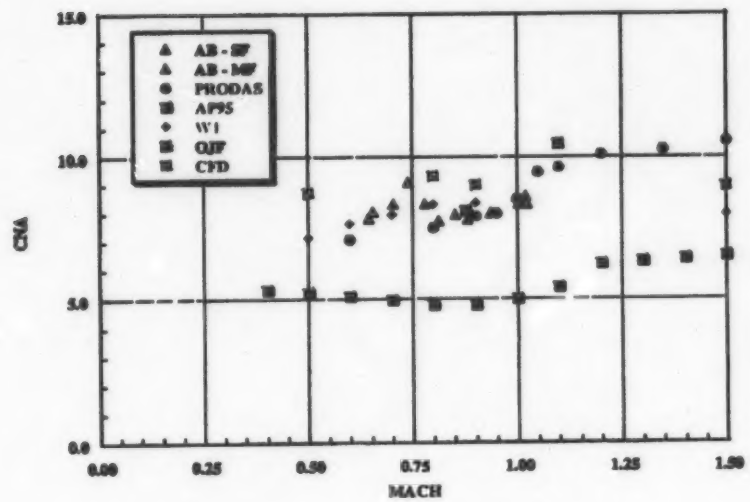

Fig. C1 b) Normal force coefficient slope

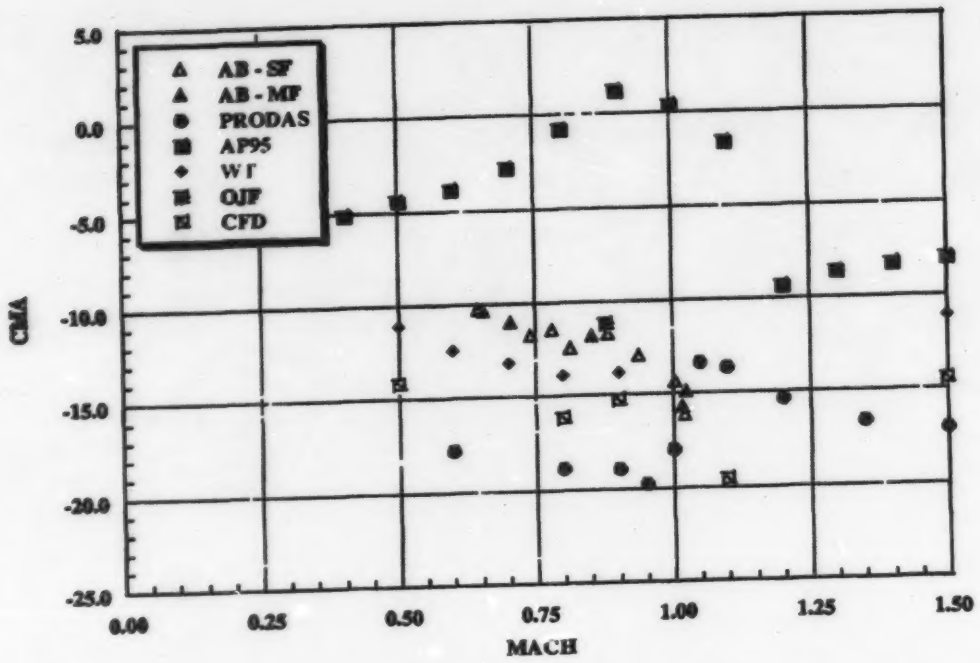

Fig. C1 d) Pitch moment coefficient slope

UNCLASSIFIED

INTERNAL DISTRIBUTION

DREV TR – 2000-115

1 – Director General

1 - Deputy Director General

1 - Chief Scientist

6 - Document Library

1 - A. Dupuis (author)

1 - F. Lesage

1 - É. Fournier

1 - A. Jeffrey

1 - G. Dumas

1 - R. Delagrave

1 - G. Bérubé

1 - M. Lauzon

1 - P. Harris

1 - Maj. Côté

1 - L. Audet

UNCLASSIFIED

EXTERNAL DISTRIBUTION

DREV TR 2000-115

1 - DRDKIM

1 - DRDKIM (unbound copy)

1 - DRDC

1 - DSAL

1 - DLR

1 - DAR 5

1 - DNR

1 - DSAA

1 - DSAM

1 - DAEPM (FT) 3

1 - DTA

1 - DTA 3-4

1 - DAPM (ES) 4-3

2 - DRES

1 - CEEM - V

1 - AETE

1 – WSM det Mirabel/SE 6

1- Mr. A. Bernier
SNC TEC .
Usine Le Gardeur
5, montée des Arsenaux
Le Gardeur, Québec
J5Z 2P4

1- Mr. N. Stathopoulos
Dept. 775
Bombardier Aerospace
1800 Marcel Laurin Blvd
St-Laurent, QC
H4R 1K2

1- Mr. N. Tang
High Speed Aerodynamic Laboratory
Institute for Aerospace Research
National Research Council Canada
Montreal Road
Ottawa, Ontario
K1A 0R6

SANS CLASSIFICATION

COTE DE SÉCURITÉ DE LA FORMULE
(plus haut niveau du titre, du résumé ou des mots-clefs)

FICHE DE CONTRÔLE DU DOCUMENT

1. PROVENANCE (le nom et l'adresse)	2. COTE DE SÉCURITÉ (y compris les notices d'avertissement, s'il y a lieu)
CRDV	UNCLASSIFIED

3. TITRE (Indiquer la cote de sécurité au moyen de l'abréviation (S, C, R ou U) mise entre parenthèses, immédiatement après le titre.)
Aerodynmic Characteristic of the BDU-5002/B MOD 1 Bomb at Subsonic and Transonic Velocities fromAerobellistic Range Free-Fligth Tests

4. AUTEURS (Nom de famille, prénom et initiales. Indiquer les grades militaires, ex.: Bleau, Maj. Louis E.)
A. Dupuis

5. DATE DE PUBLICATION DU DOCUMENT (mois et année)	6a. NOMBRE DE PAGES	6b. NOMBRE DE REFERENCES
Juin 2000	80	16

7. DESCRIPTION DU DOCUMENT (La catégorie du document, par example rapport, note technique ou mémorandum. Indiquer les dates lorsque le rapport couvre une période définie.)
rapport

8. PARRAIN (le nom et l'adresse)
DTA NDHQ

9a. NUMÉRO DU PROJET OU DE LA SUBVENTION (Spécifier si c'est un projet ou une subvention)	9b. NUMÉRO DE CONTRAT
3ec16	

10a. NUMÉRO DU DOCUMENT DE L'ORGANISME EXPÉDITEUR	10b. AUTRES NUMÉROS DU DOCUMENT
	N/A

11. ACCÈS AU DOCUMENT (Toutes les restrictions concernant une diffusion plus ample du document, autres que celles inhérentes à la cote de sécurité.)

- ☒ Diffusion illimitée
- ☐ Diffusion limitée aux entrepreneurs des pays suivants (spécifier)
- ☐ Diffusion limitée aux entrepreneurs canadiens (avec une justification)
- ☐ Diffusion limitée aux organismes gouvernementaux (avec une justification)
- ☐ Diffusion limitée aux ministères de la Défense
- ☐ Autres (préciser)

12. ANNONCE DU DOCUMENT (Toutes les restrictions à l'annonce bibliographique de ce document. Cela correspond, en principe, aux données d'accè au document (11). Lorsqu'une diffusion supplémentaire (à d'autres organismes que ceux précisés à la case 11) est possible, on pourra élargir le cerc de diffusion de l'annonce.)
Illimit/e

SANS CLASSIFICATION

COTE DE LA SÉCURITÉ DE LA FORMULE
(plus haut niveau du titre, du résumé ou des mots-clefs)

dod03/

SANS CLASSIFICATION

COTE DE LA SÉCURITÉ DE LA FORMULE

(plus haut niveau du titre, du résumé ou des mots-clefs)

13. SOMMAIRE (Un résumé clair et concis du document. Les renseignements peuvent aussi figurer ailleurs dans le document. Il est souhaitable que le sommaire des documents classifiés soit non classifié. Il faut inscrire au commencement de chaque paragraphe du sommaire la cote de sécurité applicable aux renseignements qui s'y trouvent, à moins que le document lui-même soit non classifié. Se servir des lettres suivantes: (S), (C), (R) ou (U). Il n'est pas nécessaire de fournir ici des sommaires dans les deux langues officielles à moins que le document soit bilingue.)

Free-flight tests were conducted in the Defence Research Establishment Valcartier (DREV) aeroballistic range on a full-scale MPB-LD (BDU-5002/B MOD 1) bomb from subsonic to transonic velocities. All the main aerodynamic coefficients and dynamic stability derivatives were very well determined using the six-degree-of-freedom single- and multiple-fit data reduction techniques. The cubic pitch moment and the cubic normal force coefficients terms, the yaw axial force term as well as induced moments were also reduced. Indraft wind tunnel and open jet facility experimental results were compared with the free flight ones. Estimates of the aerodynamic coefficients from two analytical codes and from one computational fluid dynamic analysis were compared with the free-flight results.

#514812

14. MOTS-CLÉS, DESCRIPTEURS OU RENSEIGNEMENTS SPÉCIAUX (Expressions ou mots significatifs du point de vue technique, qui caractérisent un document et peuvent aider à le cataloguer. Il faut choisir des termes qui n'exigent pas de cote de sécurité. Des renseignements tels que le modèle de l'équipement, la marque de fabrique, le nom de code du projet militaire, la situation géographique, peuvent servir de mots-clés. Si possible, on doit choisir des mots-clés d'un thésaurus, par exemple le "Thesaurus of Engineering and Scientific Terms (TESTS)". Nommer ce thésaurus. Si l'on ne peut pas trouver de termes non classifiés, il faut indiquer la classification de chaque terme comme on le fait avec le titre.)

FREE-FLIGHT TESTS
MODUDLAR PRACTICE BOMB - LOW DRAG
AERODYNAMIC COEFFICIENTS
6DOF
MLM METHODOLOGY
AEROBALLISTIC RANGE TESTS
LINEAR THEORY
BOMBS
GUN LAUNCHED
SUBSONIC
TRANSONIC
FINNED PROJECTILE
FLIGHT DYNAMICS
STABILITY
NONLINEAR AERODYNAMICS
PRODAS
AP96
CFD

SANS CLASSIFICATION

COTE DE SÉCURITÉ DE LA FORMULE

(plus haut niveau du titre, du résumé ou des mots-clefs)